Higher Order Corrections

John Campbell
University of Glasgow

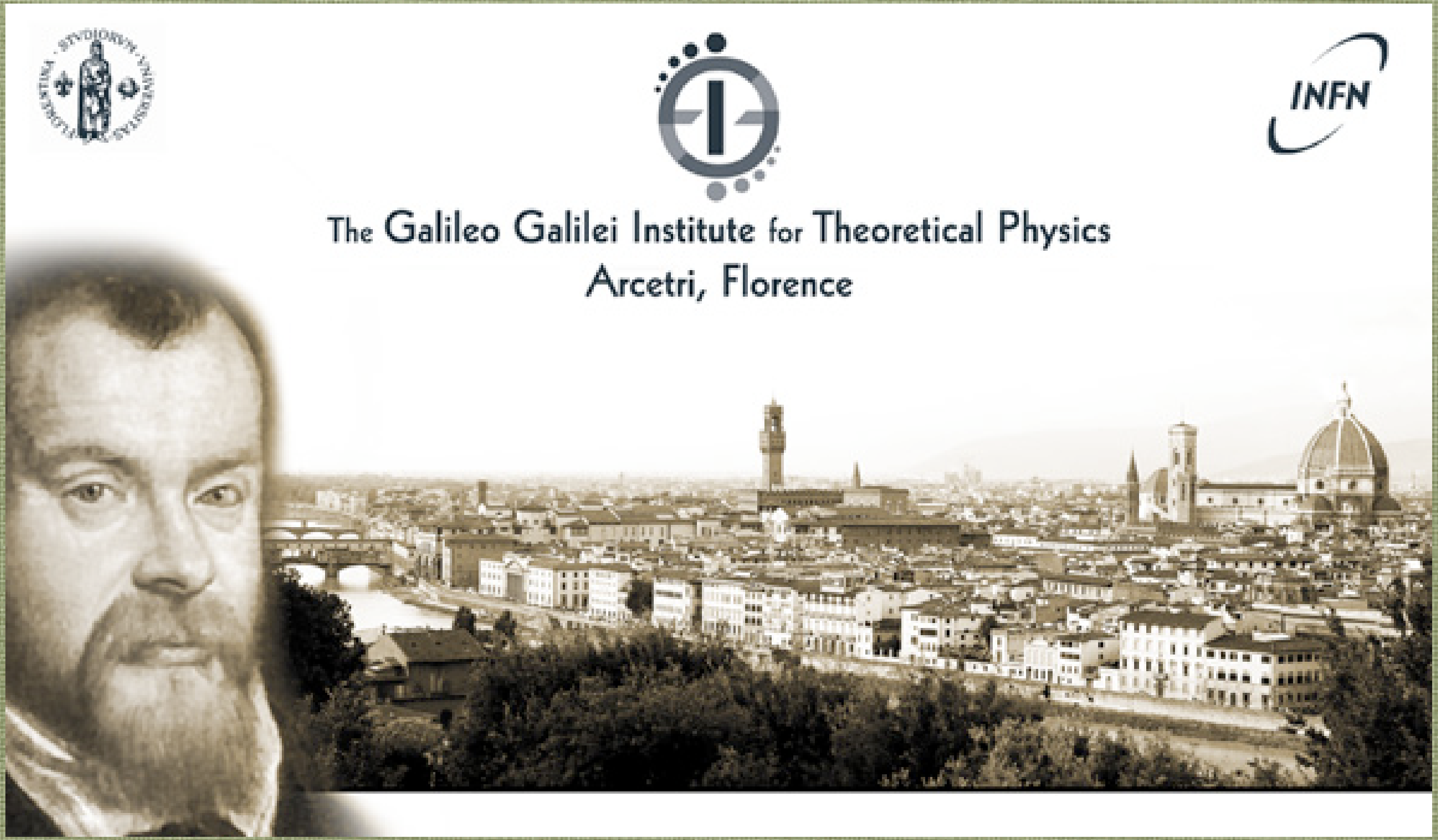

Overview of the lectures

- Structure of a partonic calculation.
- How to perform a simple NLO calculation.
- Reasons for calculating higher orders.
- Life after NLO: to NNLO and beyond.
- Examples of some state-of-the-art calculations are sprinkled throughout the lectures.

- What are the higher order corrections that I'll talk about?
- In these lectures I will be talking about corrections to hard-scattering cross sections, in particular QCD corrections.
- Since we're living in a hadron-collider dominated era (at least for now), I will concentrate on such processes.

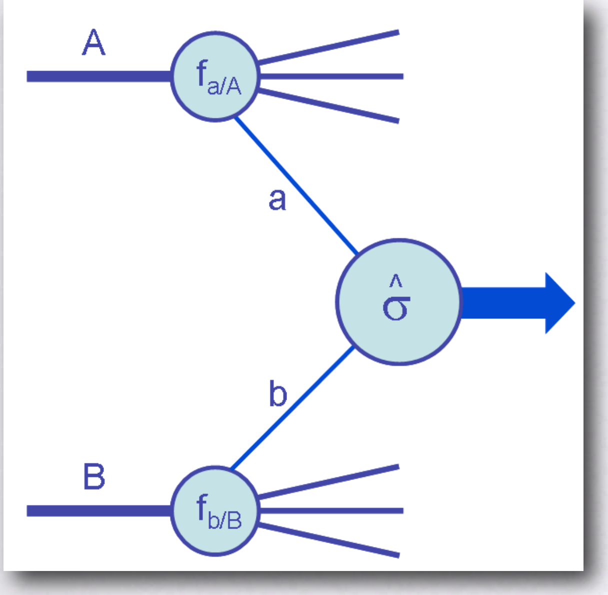

$$\sigma_{AB} = \int dx_a dx_b \; f_{a/A}(x_a, Q^2) f_{b/B}(x_b, Q^2) \; \hat{\sigma}_{ab\to X}$$

The hadronic cross section *factorizes* into a part describing the partons inside hadrons (*universal*) and another part describing the scattering of those partons (calculated case-by-case).

Any hard scale (Q^2) will do, e.g. particle with large enough mass (Drell-Yan) or high E_T object (inclusive jets).

- The presence of this scale means that the hard-scattering cross section may be calculated as a perturbative expansion, because of asymptotic freedom.
- I will be discussing an expansion in the strong coupling α_s because it plays the dominant (but not the only) role in higher order corrections:

$$\hat{\sigma}_{ab\to X} = \hat{\sigma}^{(0)}_{ab\to X} + \alpha_s(Q^2)\hat{\sigma}^{(1)}_{ab\to X} + \alpha_s(Q^2)\hat{\sigma}^{(1)}_{ab\to X} + \ldots$$

LO/tree level/Born NLO/1-loop NNLO/2-loop

- A quick word about subjects that are important, but which I won't cover.
- The other side of the coin is *soft* scattering processes. Although in principle described by the same theory of QCD, the level of understanding is much less compared with what I'll discuss here.
- Such processes are important, for instance when:
    - determining the total cross section;
    - predicting properties of the underlying event;
    - understanding multiple interactions.

c.f. the lectures of Frank Krauss

- These are all dominated by non-perturbative effects that are relatively poorly understood and in practice are often only modelled.
- Of course, in order to make sense of the wealth of data that will be available we must have both hard and soft physics under control.

Here, I'll concentrate on aspects of pQCD.

Some material is borrowed from a recent IOP review paper.

INSTITUTE OF PHYSICS PUBLISHING — REPORTS ON PROGRESS IN PHYSICS

Rep. Prog. Phys. **70** (2007) 89–193 — doi:10.1088/0034-4885/70/1/R02

Hard interactions of quarks and gluons: a primer for LHC physics

J M Campbell[1], **J W Huston**[2] and **W J Stirling**[3]

[1] Department of Physics and Astronomy, University of Glasgow, Glasgow G12 8QQ, UK
[2] Department of Physics and Astronomy, Michigan State University, East Lansing, MI 48840, USA
[3] Institute for Particle Physics Phenomenology, University of Durham, Durham DH1 3LE, UK

- Before discussing higher order corrections, here's a recap of the procedure for LO calculations.

$$\sigma_{AB} = \int dx_a dx_b \; f_{a/A}(x_a, Q^2) f_{b/B}(x_b, Q^2) \; \hat{\sigma}_{ab \to X}$$

1. Identify the leading-order partonic process that contributes to the hard interaction producing *X*.

2. Calculate the corresponding matrix elements.

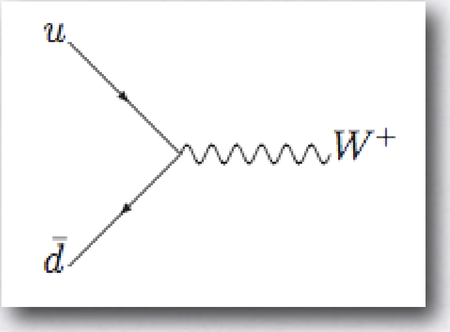

usually a tree diagram, e.g. Drell-Yan

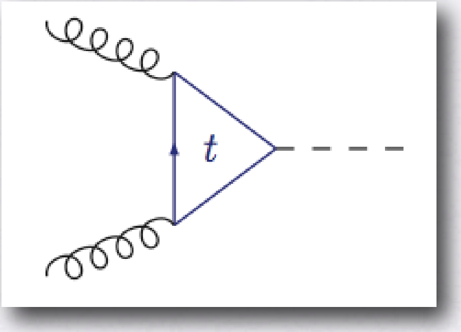

... but not always, e.g. Higgs from gluon fusion

3. Combine with appropriate combinations of pdfs for the initial-state partons *a* and *b*.

4. Perform a numerical integration over the energy fractions x_a, x_b and the phase-space for the state *X*.

- The NLO correction comes from combinations of diagrams that introduce an additional factor of α_s .

- These contributions fall into two categories, which can be illustrated simply by considering Drell-Yan production.

REAL radiation diagrams

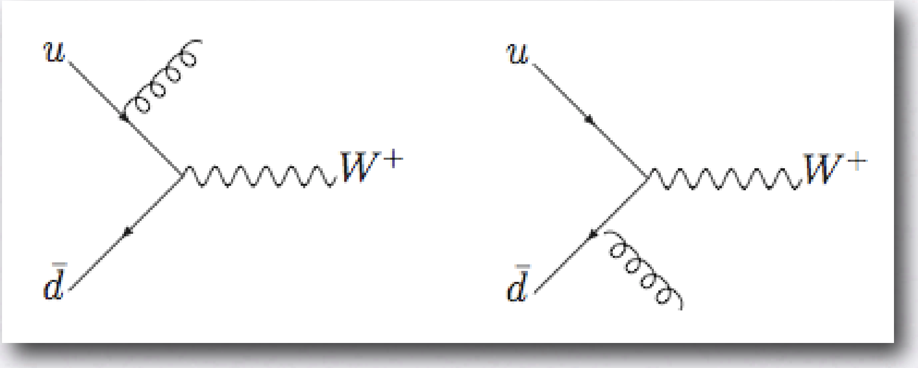

an additional gluon is radiated and present in the final state; in general there are contributions from additional quarks too

the square of the amplitude appears in the expansion

VIRTUAL radiation or ONE-LOOP diagrams

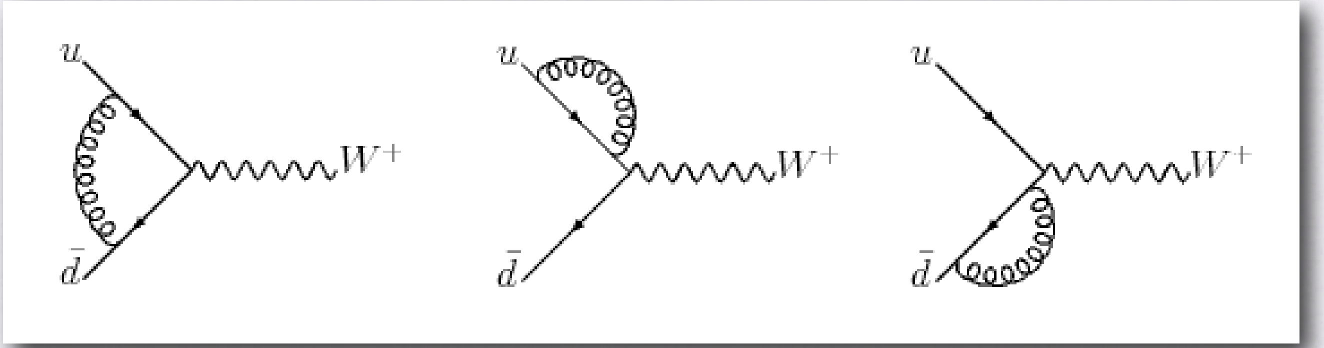

the additional radiation is emitted and reabsorbed internally

it is the interference of these diagrams with the LO ones that enters

- The evaluation of each of these contributions can be performed using a well-defined procedure that, unfortunately, leads to considerable complications.
- These complications mean that the evaluation of NLO corrections has, so far, eluded a solution via algorithmic methods (c.f. the plethora of leading order tools that F. Krauss has discussed).
- We will consider each contribution in turn.

- After straightforward application of the Feynman rules, the squared matrix elements for the real diagrams takes the form:

$$|\mathcal{M}^{u\bar{d}\to W+g}|^2 \sim g^2 \left(\frac{\hat{t}^2 + \hat{u}^2 + 2Q^2\,\hat{s}}{\hat{t}\hat{u}} \right),$$

  where the invariants are defined by: $\hat{s} = s_{u\bar{d}},\ \hat{t} = s_{ug},\ \hat{u} = s_{\bar{d}g}$.

- These must be combined with the corresponding phase space integral for a 2 →2 scattering. This contains an integral of the form,

$$\int d^4 p_g\, \delta(p_g^2) \to \int \frac{d^3\vec{p}_g}{2E_g} \propto \int E_g\, dE_g\, d\cos\theta_g$$

  where we've used the fact that the gluon is massless and where θ_g represents the orientation of the gluon w.r.t. an arbitrary set of axes.

- Taking advantage of the fact that actually all the partons are massless we can write out the invariants in terms of energies and angles, so that:

$$\hat{t} = 2E_u E_g(1 - \cos\theta_{ug}), \quad \hat{u} = 2E_{\bar{d}} E_g(1 - \cos\theta_{\bar{d}g}) \ .$$

- We can then see that, combining the final term of the ME and PS, we have:

$$\frac{g^2}{2} \int \left(\frac{Q^2 \hat{s}}{E_u E_{\bar{d}}} \right) \frac{dE_g\, d\cos\theta_g}{E_g(1 - \cos\theta_{ug})(1 - \cos\theta_{\bar{d}g})}$$

logarithmic singularities as
$E_g \to 0$, $\cos\theta_{ug} \to 1$ and $\cos\theta_{dg} \to 1$

- The divergence as $E_g \to 0$ corresponds to the gluon becoming *soft*.
- The other two divergences represent the gluon travelling exactly *collinear* to the incoming up and anti-down quarks.
- Approaching both of these limits, the physical picture of the final state looks identical to the one at LO. In a detector with finite resolution that couldn't detect close to the beam, we wouldn't be able to tell them apart.
- This too is borne out by the calculation. The matrix element that is left over is exactly the LO one.
- This is easiest to see by considering the soft limit.

kinematics with all particles outgoing: $$p_u + p_{\bar{d}} + p_W + p_g = 0$$

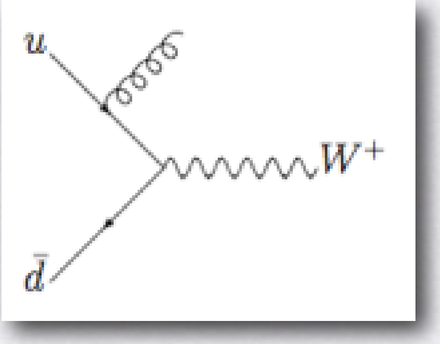

$$\left[\bar{u}(p_{\bar{d}})\gamma^\mu \frac{(-p_u - p_g)}{(p_u+p_g)^2}\gamma^\alpha u(p_u)\right] V_\mu(p_W)\epsilon_\alpha(p_g)$$
$$\to \left(\frac{-p_u\cdot\epsilon(p_g)}{p_g\cdot p_u}\right)\left[\bar{u}(p_{\bar{d}})\gamma^\mu u(p_u)\right] V_\mu(p_W)$$

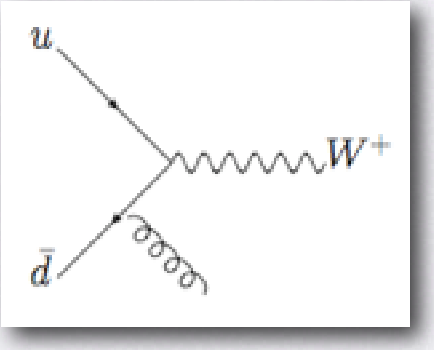

$$\left[\bar{u}(p_{\bar{d}})\gamma^\alpha \frac{(p_{\bar{d}} + p_g)}{(p_{\bar{d}}+p_g)^2}\gamma^\mu u(p_u)\right] V_\mu(p_W)\epsilon_\alpha(p_g)$$
$$\to \left(\frac{p_{\bar{d}}\cdot\epsilon(p_g)}{p_g\cdot p_{\bar{d}}}\right)\left[\bar{u}(p_{\bar{d}})\gamma^\mu u(p_u)\right] V_\mu(p_W)$$

(in the soft limit)

- Summing the diagrams, in the soft limit the amplitude is proportional to,

$$\epsilon(p_g) \cdot \left(\frac{p_{\bar{d}}}{p_g \cdot p_{\bar{d}}} - \frac{p_u}{p_g \cdot p_u} \right) \underbrace{\left[\bar{u}(p_{\bar{d}}) \gamma^\mu u(p_u)\right] V_\mu(p_W)}_{\text{LO amplitude}}$$

- Moreover, we can see the singular factor that emerges when we square the matrix element. It is just,

$$\sum_{\text{spins}} \epsilon_\mu(p_g) \epsilon^\star_\nu(p_g) \left(\frac{p_{\bar{d}}}{p_g \cdot p_{\bar{d}}} - \frac{p_u}{p_g \cdot p_u} \right)^\mu \left(\frac{p_{\bar{d}}}{p_g \cdot p_{\bar{d}}} - \frac{p_u}{p_g \cdot p_u} \right)^\nu$$

$$= \frac{2 p_u \cdot p_{\bar{d}}}{p_g \cdot p_{\bar{d}} \, p_g \cdot p_u}$$

using the usual identity to sum over gluon polarizations and the fact that the quarks are massless

- This factorization into an *eikonal factor* multiplied by the LO matrix elements is in fact universal.

- This is clear because the only diagrams which are singular in the soft limit are ones which emit the gluon at the end of a line (propagators are just scalar products involving the gluon momentum).

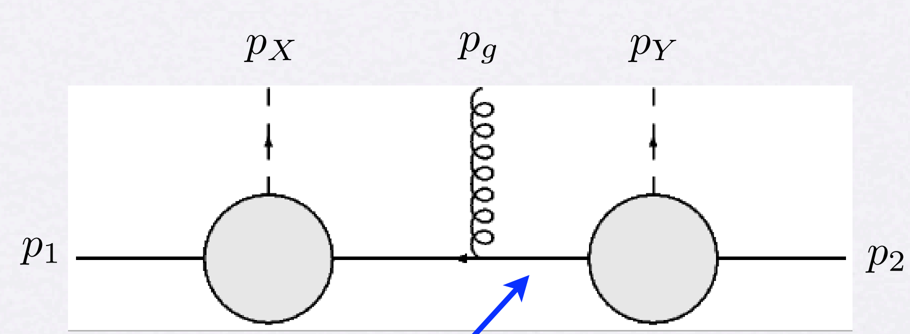

$$\frac{1}{(p_1 + p_X + p_g)^2} = \frac{1}{p_X^2 + 2 p_1 \cdot p_X + \ldots}$$

- Moreover, in our example we only relied on commuting gamma matrices at the end of a spinor line - not on the rest of the structure of the diagrams.

- The matrix element undergoes a similar factorization in the other singular cases, when the gluon is collinear to one of the quarks.

- Suppose *u* and *g* become collinear, i.e.

$$Q = p_u + p_g \quad \text{with} \quad p_u = zQ, \; p_g = (1-z)Q$$

- In that limit, the invariants can be replaced according to,

$$\hat{s} = s_{u\bar{d}} \to z s_{Q\bar{d}} \qquad \hat{u} = s_{\bar{d}g} \to (1-z) s_{Q\bar{d}} \qquad Q^2 \to s_{Q\bar{d}}$$

so that the matrix element becomes,

$$|\mathcal{M}^{u\bar{d}\to W+g}|^2 \sim g^2 \left(\frac{\hat{t}^2 + \hat{u}^2 + 2Q^2\,\hat{s}}{\hat{t}\hat{u}} \right) \longrightarrow \frac{g^2}{s_{ug}} \left((1-z) s_{Q\bar{d}} + \frac{2 s_{Q\bar{d}} \times z s_{Q\bar{d}}}{(1-z) s_{Q\bar{d}}} \right)$$

$$= s_{Q\bar{d}} \times \frac{g^2}{s_{ug}} \left(\frac{1+z^2}{1-z} \right)$$

in the limit that $s_{ug} \to 0$

LO matrix element squared

Altarelli-Parisi splitting function, $P_{qq}(z)$

- These collinear and soft singularities are a general feature of the real emission diagrams.

- Their effects must be included in a complete NLO calculation. We'll now discuss how that can be done.

- Usually we expose the singularities by using *dimensional regularization* to move away from exactly four dimensions.
- For instance, setting *d=4-2*ϵ changes our phase-space measure:

$$\int d^4 p_g \longrightarrow \int d^{4-2\epsilon} p_g \longrightarrow \int E_g^{1-2\epsilon} dE_g \, d^{2-2\epsilon}\Omega$$

- It also changes our matrix elements via the gamma matrix algebra. It actually introduces finite terms that we're not worried about for now.
- The change in measure means that the integrals are no longer logarithmically divergent, e.g. for the soft integral:

$$\int \frac{1}{E_g^2} \times E_g^{1-2\epsilon} dE_g = -\frac{1}{2\epsilon} E_g^{-2\epsilon}$$

the divergences appear as poles in the regulating parameter ϵ

- At the end of the calculation we'd like to return to reality by taking the limit ϵ→0, but for now we'll just have to live with the divergence.
- In simple cases (such as ones involving only a few particles) it's possible to perform the whole phase-space integration analytically.
- In general though, this is not the case. The phase-space is too complicated and there are too many singular regions.
- In addition, we'd like to apply experimental cuts (for instance, to identify jets or to reduce backgrounds) that are impossible to incorporate analytically.

- In that case we need an alternative strategy. The usual approach is to isolate the singular regions of phase-space and try to extract the divergent pieces in analytic form.
- When the matrix elements are not singular, the phase-space can be safely integrated numerically.
- There are two methods that are widely used in existing NLO calculations. They both rely on the fact that, in the singular regions, both the phase-space and the matrix elements factorize against universal functions.

phase-space slicing	Giele, Glover and Kosower, 1980; Keller and Laenen, 1999; Harris and Owens, 2002.
subtraction	Ellis, Ross and Terrano, 1981; Catani and Seymour, 2002.

- I'll briefly describe both approaches with reference to a toy integral:

$$\mathcal{I} = \int_0^1 \frac{dx}{x} x^{-\epsilon} \mathcal{M}(x)$$

x controls the approach to the singular region, c.f. the gluon energy

M(x) represents the real matrix elements, with M(0) the lowest order

- I'll then look at the subtraction method in more detail.

- In the slicing approach, an additional theoretical parameter (δ) is introduced which is used to define the singular region.
- Close to the singular region, the matrix elements are approximated by the leading order ones.
- In our toy model, this means choosing δ«1 and approximating *M(x)* by *M(0)* when *x*<δ.
- In that case we can split the integral into two regions thus:

$$\begin{aligned}\mathcal{I} &= \mathcal{M}(0)\int_0^\delta \frac{dx}{x}x^{-\epsilon} + \int_\delta^1 \frac{dx}{x}x^{-\epsilon}\mathcal{M}(x) \\ &= -\frac{1}{\epsilon}\delta^{-\epsilon}\mathcal{M}(0) + \int_\delta^1 \frac{dx}{x}\mathcal{M}(x) \\ &= \left(-\frac{1}{\epsilon} + \log\delta\right)\underbrace{\mathcal{M}(0) + \int_\delta^1 \frac{dx}{x}\mathcal{M}(x)}_{\text{finite and ready to be integrated numerically}}\end{aligned}$$

dropping the regularising term in the second integral because it's finite

isolated singularity

- The final result should be independent of δ, via an implicit cancellation of logarithms between the exposed log and the lower limit of the integral.
- Therefore there is a tension between retaining a good approximation (wanting small δ) and reducing numerical log-cancellations (large δ).

- e.g. *Wbb* production (with massive *b*-quarks) at NLO. Actually uses two cutoffs, one for soft (δ_s) and one for collinear (δ_c) singularities.

Febres Cordero, Reina, Wackeroth, 2006

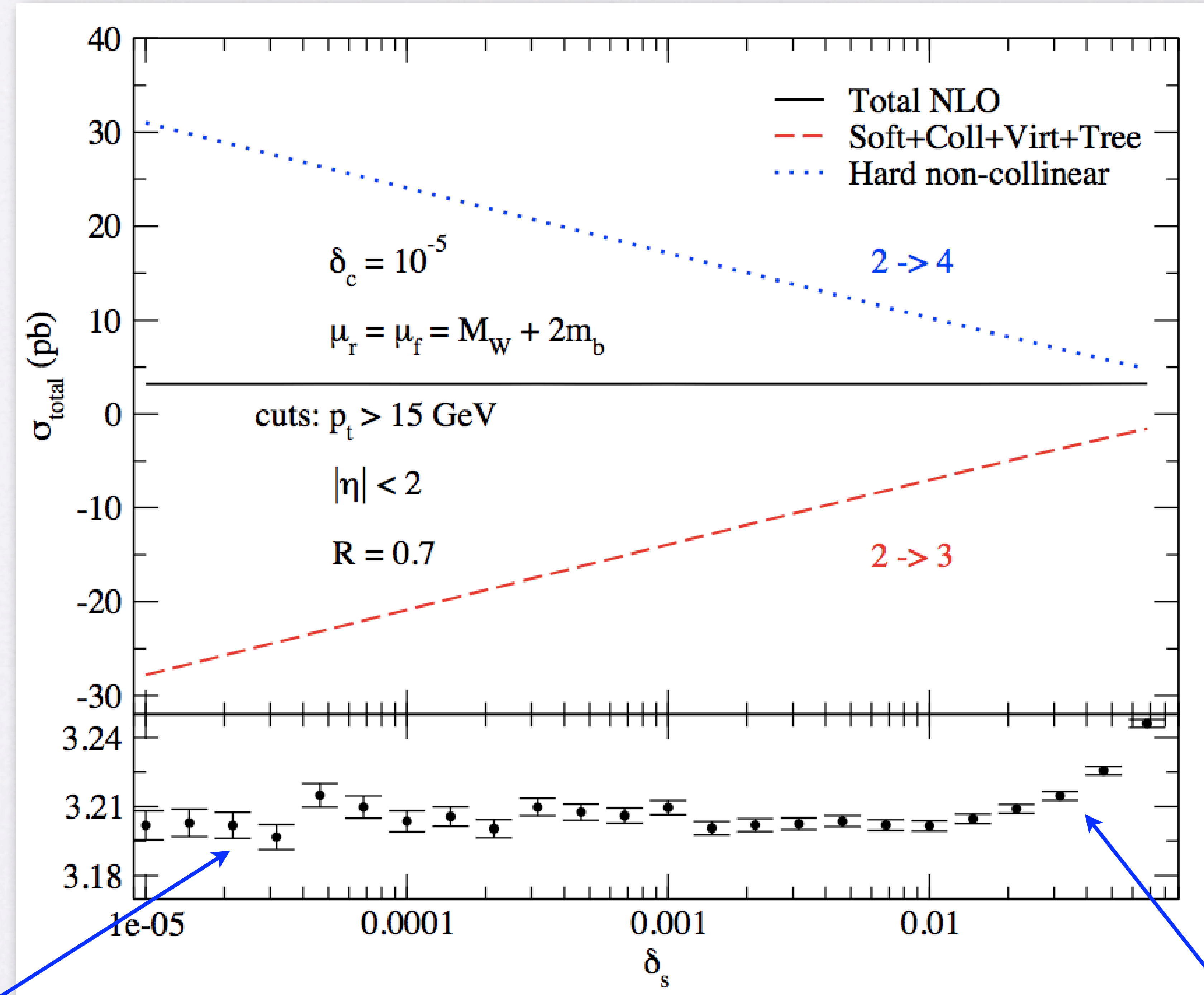

numerical instability

large logarithms

- The method of subtraction proceeds by subtracting from the integrand, in each singular region, a local counterterm with exactly the same singular behaviour.

- In our toy integral, the counterterm is obvious:

$$\mathcal{I} = \int_0^1 \frac{dx}{x} x^{-\epsilon} \underbrace{[\mathcal{M}(x) - \mathcal{M}(0)]}_{\text{local counterterm}} + \mathcal{M}(0) \int_0^1 \frac{dx}{x} x^{-\epsilon}$$

$$= \underbrace{\int_0^1 \frac{dx}{x} [\mathcal{M}(x) - \mathcal{M}(0)]}_{\text{suitable for numerical integration}} - \underbrace{\frac{1}{\epsilon}\mathcal{M}(0)}_{\text{isolated singularity}}$$

- This procedure appears to be straightforward, but is in fact more tricky than it seems at first sight.

- First, a cutoff is still needed in practise. For numerical stability, it is still impractical to integrate the subtracted singularity completely (to zero, in our toy example).

- In addition, the trick here is to construct the singular terms in such a manner that they are both universal and readily integrated analytically.

- Such a formulation is provided by the *dipole subtraction* procedure.

- The dipole subtraction method introduces local counterterms for each of the collinear singularities.
- The method harks back to the earliest form of subtraction in which the eikonal terms representing the soft singularities are partional-fractioned:

$$\frac{p_a \cdot p_b}{p_g \cdot p_a \, p_g \cdot p_b} = \frac{1}{p_g \cdot p_a} \frac{p_a \cdot p_b}{(p_g \cdot p_a + p_g \cdot p_b)} + \frac{1}{p_g \cdot p_b} \frac{p_a \cdot p_b}{(p_g \cdot p_a + p_g \cdot p_b)}$$

dipole 1: (*a*,*g*,*b*) dipole 2: (*b*,*g*,*a*)

- The result is two collinear singularities, or dipoles. They are described in terms of the three partons - emitter, emitted and spectator.
- In general the matrix elements can be written as a sum over many eikonal terms. Hence the subtraction of singularities corresponds to a sum over many dipole counterterms.
- The method relies on a redefinition of the momenta in the subtracted matrix element such that the phase space can be exactly factorized.
- The details of the transformations of the momenta depend on whether the emitted and spectator partons are in the initial or final state of the process. Hence there are four different types of dipole.

- e.g. “final-final” singularity with final state emitter parton *a* and spectator *b*.
- Define transformed momenta for the emitter and spectator by:

$$\tilde{p}_a^\mu = p_a^\mu + p_g^\mu - \frac{y}{1-y}\, p_b^\mu, \qquad \tilde{p}_b^\mu = \frac{1}{1-y}\, p_b^\mu$$

with the additional variable *y* given by, $y = \dfrac{p_a \cdot p_g}{(p_a \cdot p_g + p_b \cdot p_g + p_a \cdot p_b)}$.

- These are the momenta that appear in the matrix elements of the counterterms. They allow the phase-space to be factorized via:

$$d\mathrm{PS}_n(\ldots p_a, p_g, p_b, \ldots) = d\mathrm{PS}_{n-1}(\ldots \tilde{p}_a, \tilde{p}_b, \ldots) \times d\mathrm{PS}_1(p_g)$$

- This is possible because the kinematics are implemented exactly:

$$p_a + p_g + p_b = \tilde{p}_a + \tilde{p}_b$$

momentum conservation

$$\tilde{p}_a^2 = \tilde{p}_b^2 = 0$$

on-shell relations preserved

(c.f. the simplest formulation, defined without reference to a spectator parton)

- Slightly different transformations are used for each type of dipole, but these features are common throughout.

- The actual subtraction term for the "final-final" dipole corresponding to the splitting $q \to qg$ is: $$\frac{1}{2p_a \cdot p_g}\left(\frac{2}{1-z(1-y)} - 1 - z - \epsilon(1-z)\right)$$
where z is the fractional momentum as before, $z = \dfrac{p_a \cdot p_b}{p_a \cdot p_b + p_g \cdot p_b}$.

- It looks much like the regular splitting function, which it maps onto in the limit $y \to 0$, but reproduces the correct form of the partial-fractioned eikonal.

- The corresponding phase space that is factored out takes the form,
$$\int_0^1 dy\, y^{-1-\epsilon}(1-y)^{1-2\epsilon} \int_0^1 dz\, z^{-\epsilon}(1-z)^{-\epsilon}$$
where we've absorbed the collinear propagator factor ($1/y$) from the dipole.

- The singularities are manifest as $y \to 0$ and $z \to 1$, but are regularized by keeping away from four dimensions as before.

- The integrals can be performed, yielding:
$$\int [\text{dipole}]\, dPS_1 = \frac{1}{\epsilon^2} + \frac{3}{2\epsilon} + 5 - \frac{\pi^2}{2} \ .$$

- Similar results can be tabulated for all the other combinations of initial and final particles and flavours of parton.

- A more complicated example: W+jet production. The real radiation corrections to this process include diagrams with a W and two gluons.

$t^B t^A$

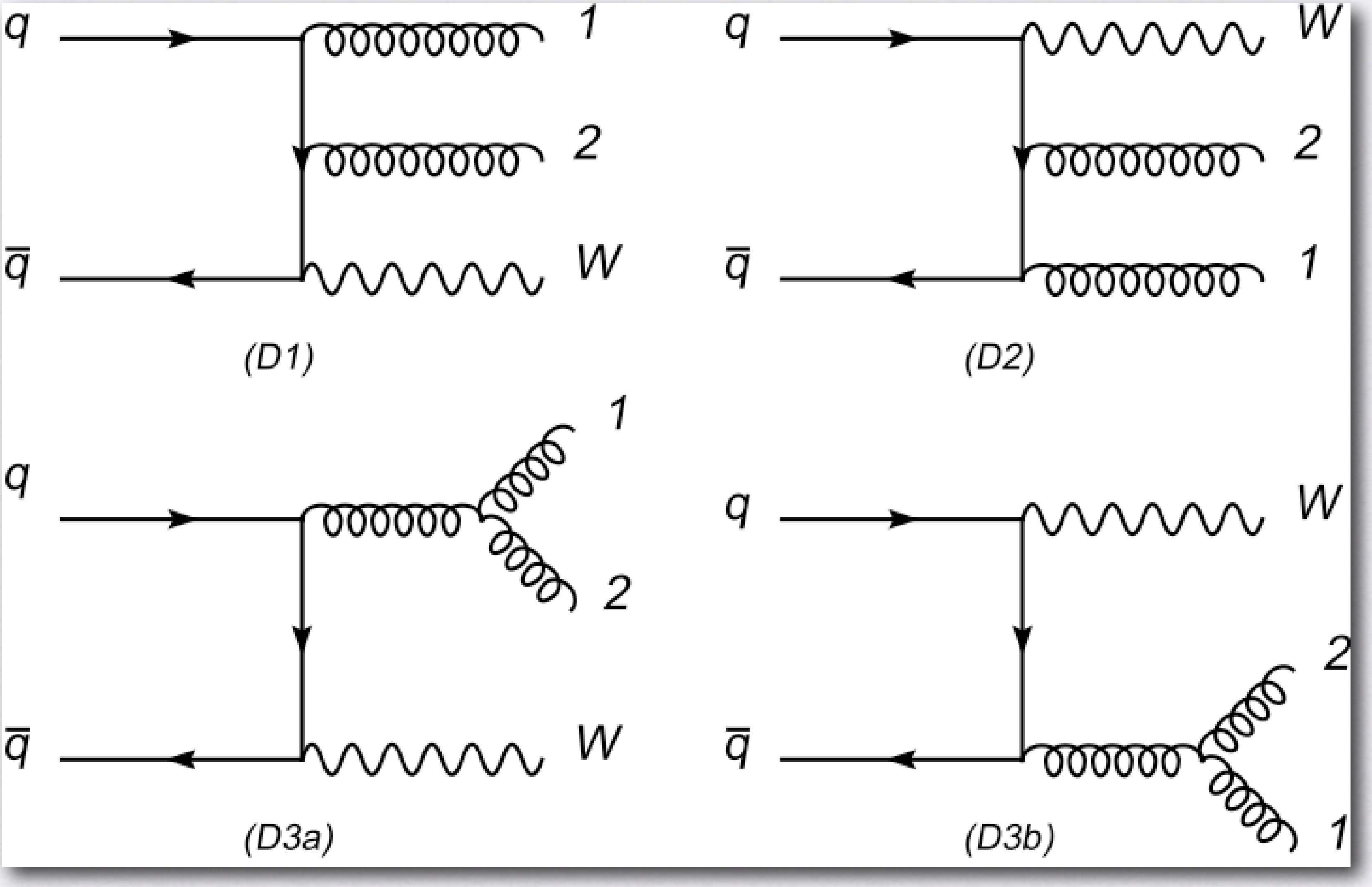

$t^A t^B$

$$if^{ABC} t^C = (t^A t^B - t^B t^A)$$

- Let's look at the singularity structure of the matrix elements when gluon 1 becomes soft. These diagrams are the only relevant ones because they include gluon 1 adjacent to an external particle.

- The presence of two gluons ensures non-trivial colour structure.

- The amplitude can thus be written as,

$$\mathcal{M}^{q\bar{q}\to Wgg} = t^A t^B \underbrace{(D_2 + D_3)} + t^B t^A \underbrace{(D_1 - D_3)}$$

colour matrices factored out

kinematic structure only

- The remaining stripped-out structures are *colour-ordered amplitudes*.

- It is then straightforward to square up the colour matrices using, e.g. the Fierz identity for the colour matrices.

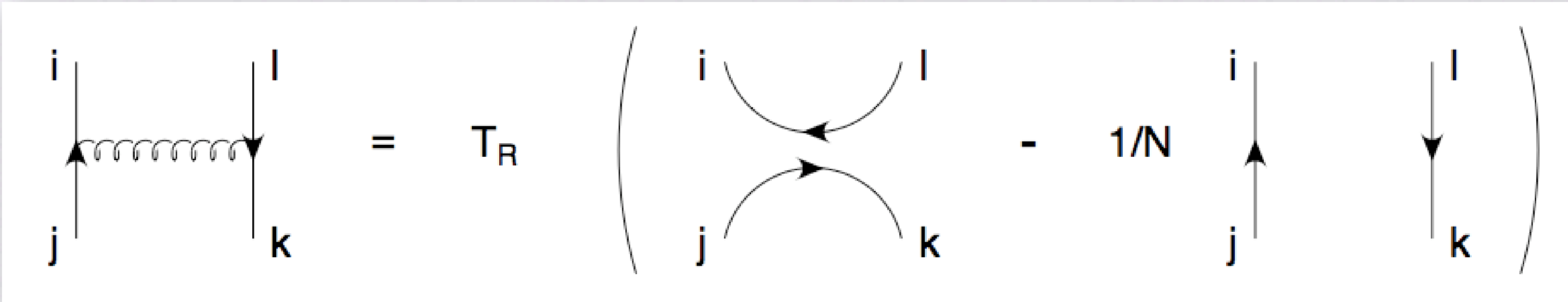

- The result (after a little bit of algebra) is,

$$|\mathcal{M}^{q\bar{q}\to Wgg}|^2 = \frac{C_F N^2}{2}\left[|D_2 + D_3|^2 + |D_1 - D_3|^2 - \frac{1}{N^2}|D_1 + D_2|^2\right].$$

- It is these squared colour-ordered amplitudes that factorize simply in the soft and collinear limits. They represent the proper generalization of our simple example, where the full matrix element factored exactly over the LO.

$$|\mathcal{M}^{q\bar{q}\to Wgg}|^2 \xrightarrow{\text{soft}} \frac{C_F N^2}{2}\left[[q\ p_2] + [p_2\ \bar{q}] - \frac{1}{N^2}[q\ \bar{q}]\right]\mathcal{M}^{q\bar{q}\to Wg}.$$

with our usual eikonal factor, $[a\ b] \equiv \dfrac{a\cdot b}{p_1\cdot a\ p_1\cdot b}$

- These singularities can be interpreted in terms of lines of colour flow along the quarks and gluons in the LO matrix element. The colour-connected partons are the emitter and spectator for the emitted gluon.

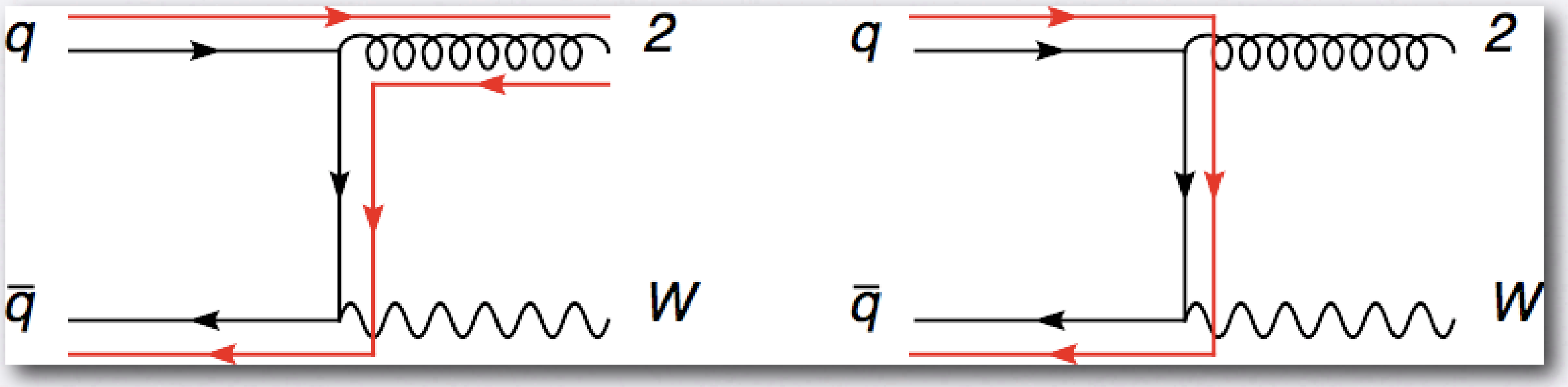

- The leading term in N contains singularities along two lines, connecting gluon 2 to the quark and anti-quark respectively.

- The sub-leading term has a singularity on a line of colour flow straight along the quark line. The reason is that the matrix elements for the sub-leading term are just the same (modulo overall coupling factors) as those for the emission of two photons from a quark line.

- In parton shower Monte Carlos such as HERWIG and PYTHIA the gluon emission in the shower proceeds along the lines of leading colour flow.

- Using the subtraction method, the eikonal pattern is readily interpreted in terms of dipoles:

$$\frac{C_F N^2}{2}\left[[q\ p_2] + [p_2\ \bar{q}] - \frac{1}{N^2}[q\ \bar{q}]\right]$$

2 dipoles (initial-final and final-initial)

2 more similar dipoles

2 initial-initial dipoles

note: many dipoles, each with their own kinematics and ME's

Real radiation summary

- The real radiation diagrams contain soft and collinear singularities. They can be readily identified from the diagrams themselves, particularly with the help of colour decomposition.
- The singularities take the form of universal factors multiplied by the LO matrix elements.
- This factorization of matrix elements (and phase space) is exploited by the techniques of *slicing* and *subtraction*. Both methods effectively isolate the singularities. As the numbers of partons in the final state grows, this procedure becomes more complicated because more singular regions must be handled in this way (e.g. must calculate many dipole terms).
- They are extracted analytically using dimensional regularization, resulting in poles in the parameter ϵ.
- The remainder of the phase space integration can be performed numerically. This procedure is well-established and is implemented in many parton-level Monte Carlo programs.
- Now we must turn to the issue of the remaining poles and how they are accounted for in the full calculation. To see this, we'll now move on to discuss the virtual diagrams.

- Let's return to W production, where the most complicated diagram (and, in fact, usually the only one) is the vertex correction.

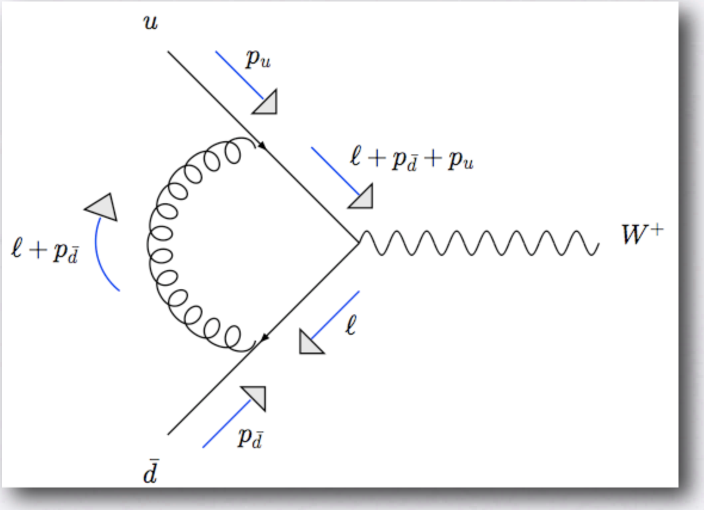

- An arbitrary loop momentum ℓ is introduced which, nevertheless, satisfies momentum conservation at each vertex. It is integrated out in the evaluation of the amplitude:

$$\int \frac{d^4\ell \quad \mathcal{N}}{\ell^2(\ell+p_{\bar{d}})^2(\ell+p_{\bar{d}}+p_u)^2}$$

  where the propagators in the loop make up the denominator and the numerator factor results from the Dirac structure of the matrix elements,

$$\mathcal{N} = [\bar{u}(p_{\bar{d}})\gamma^\alpha \not{\ell}\gamma^\mu(\not{\ell}+\not{p}_{\bar{d}}+\not{p}_u)\gamma_\alpha u(p_u)]\, V_\mu(p_W)\,.$$

- The evaluation of these integrals in the general case is highly non-trivial and for a long time has been a major challenge in generating NLO predictions.

- The integrals can be classified according to the form of the propagators and the powers of the loop momentum that are present in the numerator. Life would be much easier if we only had scalar propagators and couplings!

- Inspection of the denominators reveals the now-familiar problems. They are best seen by shifting the loop momentum:

$$\ell^2(\ell+p_{\bar{d}})^2(l+p_{\bar{d}}+p_u)^2 \longrightarrow \ell^2(\ell-p_{\bar{d}})^2(l+p_u)^2 \qquad [\ell \to \ell - p_{\bar{d}}]$$

- There is a soft singularity as $\ell \to 0$ and two collinear singularities, when ℓ is proportional to either of the external momenta: $\ell \propto p_{\bar{d}}$ or $\ell \propto p_u$.

- These *infrared* singularities, just as in the real diagrams, can be handled by using dimensional regularization.

- There are further problems though, which only become apparent when considering the numerator. If we project out the loop momentum in the numerator factor,

$$\mathcal{N} = \mathcal{N}_0 + \mathcal{N}_1^{\mu}\ell_\mu + \mathcal{N}_2^{\mu\nu}\ell_\mu\ell_\nu$$

then simple power-counting shows that the final term diverges for large loop momenta, i.e. it contains an *ultraviolet* divergence.

$$\int d^4\ell \, \frac{\ell_\mu\ell_\nu}{\ell^2(\ell+p_{\bar{d}})^2(\ell+p_{\bar{d}}+p_u)^2} \longrightarrow \log(|\ell^0|) \quad \text{as } |\ell^0| \to \infty$$

- In fact, DR takes care of both of these problems at once. Formally, $\epsilon<0$ to regularize the IR divergences and $\epsilon>0$ for the UV ones.

- One finds that the UV and IR divergences are both proportional to LO, just as in the case of the real radiation diagrams.

- For simple cases (such as this vertex correction) it is straightforward to perform the integrals directly.

- The normal method is to combine the denominators with Feynman parameters and shift the loop momentum:

(Feynman parameters)

$$\frac{1}{\ell^2(\ell+p_{\bar d})^2(\ell+p_{\bar d}+p_u)^2} = 2\int_0^1 dx_1 \int_0^1 dx_2 \int_0^1 dx_3 \, \frac{\delta(x_1+x_2+x_3-1)}{\left[x_1\ell^2 + x_2(\ell+p_{\bar d})^2 + x_3(\ell+p_{\bar d}+p_u)^2\right]^3}$$

$$= 2\int_0^1 dx_1 \int_0^{1-x_1} dx_3 \, \frac{1}{(L^2-\Delta)^3}$$

$$L = \ell + (1-x_1)\, p_{\bar d} + x_3\, p_u$$

$$\Delta = -2x_1 x_3\, p_u \cdot p_{\bar d}$$

(loop momentum shift)

- The move to *d* dimensions, together with a Wick rotation, leaves the final result expressed in terms of gamma functions:

$$\int \frac{d^dL}{(2\pi)^d} \frac{1}{(L^2-\Delta)^n} = i\,\frac{(-1)^n}{(4\pi)^{d/2}} \frac{\Gamma\left(n-\frac{d}{2}\right)}{\Gamma(n)} \Delta^{d/2-n}$$

- If the loop momentum shift is substituted back into the numerator that comes from the matrix elements, all the remaining integrals can be performed in terms of beta (i.e more gamma) functions. For example,

$$\int_0^1 dx_1 \int_0^{1-x_1} dx_3 \, (-2x_1x_3\, p_u\cdot p_{\bar d})^{-1-\epsilon} = (-2p_u\cdot p_{\bar d})^{-1-\epsilon} \int_0^1 dx_1\, x_1^{-1-\epsilon}\left(-\frac{1}{\epsilon}\right) x_1^{-\epsilon}$$

$$= (-2p_u\cdot p_{\bar d})^{-1-\epsilon}\left(-\frac{1}{\epsilon}\right)\frac{\Gamma(-\epsilon)\Gamma(1-\epsilon)}{\Gamma(1-2\epsilon)} = (-2p_u\cdot p_{\bar d})^{-1-\epsilon}\left(\frac{1}{\epsilon^2}\right)\frac{\Gamma^2(1-\epsilon)}{\Gamma(1-2\epsilon)}$$

soft singularity exposed

- Terms involving an odd power of *L* vanish, by symmetry.
- The remaining term has two powers of *L* and symmetry this time simplifies the integral,

$$\int \frac{d^dL}{(2\pi)^d}\frac{L^\mu L^\nu}{(L^2-\Delta)^n} = \frac{g^{\mu\nu}}{d}\int \frac{d^dL}{(2\pi)^d}\frac{L^2}{(L^2-\Delta)^n} = \frac{g^{\mu\nu}}{d}\int \frac{d^dL}{(2\pi)^d}\left[\underbrace{\frac{1}{(L^2-\Delta)^{n-1}}}+\underbrace{\frac{\Delta}{(L^2-\Delta)^n}}\right]$$

$$= i\frac{(-1)^{n-1}}{(4\pi)^{d/2}}\frac{\Gamma\left((n-1)-\frac{d}{2}\right)}{\Gamma(n-1)}\Delta^{d/2-(n-1)} + i\frac{(-1)^n}{(4\pi)^{d/2}}\frac{\Gamma\left(n-\frac{d}{2}\right)}{\Gamma(n)}\Delta^{d/2-n+1}$$

$$= i\frac{(-1)^n}{(4\pi)^{d/2}}\frac{\Gamma\left(n-1-\frac{d}{2}\right)}{\Gamma(n)}\Delta^{d/2-n+1}\left[-(n-1)+(n-\frac{d}{2}-1)\right]$$

$$= i\frac{(-1)^n}{(4\pi)^{d/2}}\frac{\Gamma\left(n-\frac{d+2}{2}\right)}{\Gamma(n)}\Delta^{(d+2)/2-n}\left(-\frac{d}{2}\right)$$

(Generally true, not just for this special case)

i.e. apart from a trivial overall factor the term proportional to the metric tensor is actually the usual scalar integral, but in *(d+2)* dimensions.

- Inspecting the argument of the gamma function shows the presence of the UV divergence explicitly.
- In a simple calculation such as this one, all the integrals are straightforward and we are almost done. In more complicated processes, performing the FP integrals for the scalar integral is hard enough.
- One then needs a systematic way of evaluating the tensor integrals.

- A popular method is *Passarino-Veltman* reduction. Passarino, Veltman, 1979.
- First, one performs a form-factor expansion of the integral over the basis of available tensor structures, e.g.

$$\int d^d\ell \, \frac{\ell^\mu}{\ell^2(\ell+p_{\bar{d}})^2(\ell+p_{\bar{d}}+p_u)^2} = A_1\, p_{\bar{d}}^\mu + B_1\, p_u^\mu$$

$$\int d^d\ell \, \frac{\ell^\mu \ell^\nu}{\ell^2(\ell+p_{\bar{d}})^2(\ell+p_{\bar{d}}+p_u)^2} = A_2\, p_{\bar{d}}^\mu p_{\bar{d}}^\nu + B_2\, p_u^\mu p_u^\nu + C_2\, \left(p_{\bar{d}}^\mu p_u^\nu + p_u^\mu p_{\bar{d}}^\nu\right) + D_2\, g^{\mu\nu}$$

- The coefficients are then determined by contracting with external momenta and expressing the dot products in terms of the propagators, e.g.

$$\begin{aligned} A_1\, p_{\bar{d}}\cdot p_u &= \frac{1}{2}\int d^d\ell \, \frac{(\ell+p_{\bar{d}}+p_u)^2 - (l+p_{\bar{d}})^2 - 2p_u\cdot p_{\bar{d}}}{\ell^2(\ell+p_{\bar{d}})^2(\ell+p_{\bar{d}}+p_u)^2} \\ &= \frac{1}{2}\int d^d\ell \left[\underbrace{\frac{1}{\ell^2(\ell+p_{\bar{d}})^2} - \frac{1}{\ell^2(\ell+p_{\bar{d}}+p_u)^2}}_{\text{scalar integrals with one propagator removed, or “pinched” away}} - \underbrace{\frac{2p_u\cdot p_{\bar{d}}}{\ell^2(\ell+p_{\bar{d}})^2(\ell+p_{\bar{d}}+p_u)^2}}_{\text{original scalar integral}} \right] \end{aligned}$$

- In this way the tensor integrals can be reduced to combinations of already-calculated scalar integrals with the same, or fewer, propagators.
- In general it can be formulated as a matrix method in which the coefficients are found by inverting matrices of kinematic factors.

- As an example, the simplest integral is recast in terms of vectors,

$$\int d^d\ell \, \frac{\ell^\mu}{\ell^2(\ell+p_{\bar{d}})^2(\ell+p_{\bar{d}}+p_u)^2} = \begin{pmatrix} p_{\bar{d}}^\mu & p_u^\mu \end{pmatrix} \begin{pmatrix} A_1 \\ B_1 \end{pmatrix}$$

and then the two possible contractions of the loop momentum with external momenta are represented by multiplication with another vector:

$$\begin{pmatrix} 2p_{\bar{d}\,\mu} \\ 2p_{u\,\mu} \end{pmatrix} \int d^d\ell \, \frac{\ell^\mu}{\ell^2(\ell+p_{\bar{d}})^2(\ell+p_{\bar{d}}+p_u)^2} = \underbrace{\begin{pmatrix} 2p_{\bar{d}\,\mu} \\ 2p_{u\,\mu} \end{pmatrix} \begin{pmatrix} p_{\bar{d}}^\mu & p_u^\mu \end{pmatrix}}_{\text{a 2x2 matrix, G}} \begin{pmatrix} A_1 \\ B_1 \end{pmatrix}$$

- The coefficients are then given by,

$$\begin{pmatrix} A_1 \\ B_1 \end{pmatrix} = G^{-1} \begin{pmatrix} \int \frac{d^d\ell \; 2\ell\cdot p_{\bar{d}}}{(\ldots)} \\ \int \frac{d^d\ell \; 2\ell\cdot p_u}{(\ldots)} \end{pmatrix}$$

where the integrals are reduced to scalar integrals as before and the *Gram matrix G* is defined as,

$$G = \det(2p_i \cdot p_j) = \begin{pmatrix} 2p_{\bar{d}}\cdot p_{\bar{d}} & 2p_{\bar{d}}\cdot p_u \\ 2p_{\bar{d}}\cdot p_u & 2p_u\cdot p_u \end{pmatrix} .$$

- Hence the inverse matrix of kinematic factors is just:

$$G^{-1} = \frac{1}{4[p_u^2 p_{\bar{d}}^2 - (p_u\cdot p_{\bar{d}})^2]} \begin{pmatrix} 2p_u\cdot p_u & -2p_{\bar{d}}\cdot p_u \\ -2p_u\cdot p_{\bar{d}} & 2p_{\bar{d}}\cdot p_{\bar{d}} \end{pmatrix} .$$

Gram determinant

- Although this method is tried and tested, it becomes complicated for processes which involve a large number of particles and, in particular, high powers of loop momenta in the numerator.
- This can result in a proliferation of terms which can easily lead to large intermediate expressions during a calculation.
- In addition, the Gram determinants that arise when inverting the matrices can cause problems. Although individual terms in the expressions may contain high powers of this determinant in the denominator that appear to be singularities, the original integrals do not have problems in this limit.
- They vanish when two of the external momenta are degenerate; such configurations may therefore be approached within the physical PS.
- Such spurious divergences (the same sort of behaviour may occur in other kinematic regions too) can cause numerical instabilities.
- In wholly-analytic approaches to the tensor integrals this may not be too serious of a problem. Using a method that relies more on numerical techniques, this is a major concern.
- Methods have been introduced which try to deal with this problem, for example by collecting together appropriate terms which are finite as the regions are approached. Alternatively, the reduction itself can be modified to take the degeneracy into account *ab initio*.

- Going back to our example, when we put the real and virtual terms together then we have 4 contributions using the subtraction method:

REAL

$$|\mathcal{M}^{u\bar{d}\to W+g}|^2 - \sum(\text{singular})|\mathcal{M}^{u\bar{d}\to W}|^2$$

real matrix elements with singular regions subtracted, finite and integrated numerically

$$\left(\frac{2}{\epsilon^2} + \frac{3}{\epsilon} - \frac{2}{\epsilon}P_{qq} + \mathcal{O}(\epsilon^0)\right)|\mathcal{M}^{u\bar{d}\to W}|^2$$

counter-terms integrated analytically over singular phase space

VIRTUAL

$$\left(-\frac{2}{\epsilon^2} - \frac{3}{\epsilon}\right)|\mathcal{M}^{u\bar{d}\to W}|^2$$

divergences extracted from the virtual diagrams, proportional to LO

$$\mathcal{O}(\epsilon^0)$$

finite non-factorizable contributions

- The simple poles in the real and virtual contributions are equal and opposite so that they cancel in the sum. This is guaranteed by the Bloch-Nordsieck and KLN theorems, for properly defined observables in any process.
- The remaining divergence that is proportional to P_{qq} is universal and must be factored into the definition of the pdfs at NLO. When it is subtracted, a finite contribution is included that is dependent on the scheme (usually $\overline{\text{MS}}$, but sometimes DIS).
- All contributions are now suitable for inclusion in a *parton-level* Monte Carlo program that performs the phase-space integrations.

Benefits of NLO

- The most obvious effect of NLO corrections is a change in the cross section; it is not guaranteed to increase, but often it does.

- The information provided by a NLO calculation is often encapsulated by a single number: the *K-factor*, or ratio of NLO to LO cross sections.

hadron-collider process	scale	Tevatron	LHC
W production	m_W	1.33	1.15
top pairs	m_t	1.08	1.40
$W + 1$ jet ($p_T^{\text{jet}} > 20$ GeV, $\lvert\eta^{\text{jet}}\rvert < 2.5$)	m_W	1.24	1.31
weak boson fusion (m_H=120 GeV)	m_H	1.07	1.23

- The K-factor obviously depends upon the process under consideration and the collider. For more complicated final states (e.g. ones involving jets), it also depends on the cuts used to define the LO cross section.

- It can also have a non-trivial dependence on input parameters such as masses and parton distribution functions.

- In particular, it is common practice to use leading order PDFs (extracted and implemented with a 1-loop value of α_s and evolution) in the denominator and NLO PDFs (with 2-loop ...) in the numerator. This is the case for the numbers in the table above.

- The K-factor must be used with care however, since it washes out important kinematic effects that the NLO corrections introduce.

- These are the reasons that we would want to build a Monte Carlo program in the first place. Fully-analytic approaches, where tractable, are only useful for fully inclusive calculations or ones that are differential in particular variables.

- As a trivial example, consider the simplest hadron-collider process again and look at the transverse momentum of a *W* produced at the Tevatron.

- Both the LO and virtual contributions have 2→1 kinematics. By conservation of momentum, the *W* boson does not acquire any p_T.

- In the real contribution, the diagrams are 2→2 processes in which the *W* balances against a hard parton. However the counterterms must all appear in the first bin.

- Clearly no K-factor can account for this richer kinematic structure at NLO.

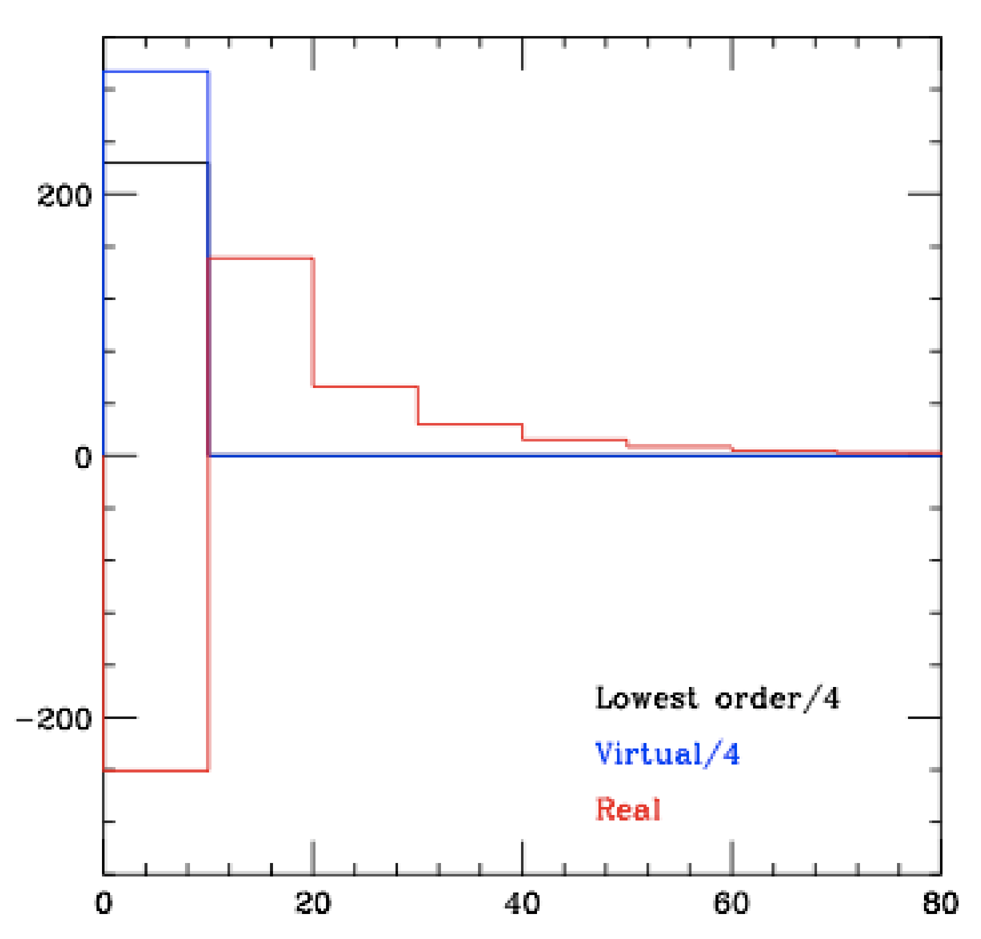

$p_T(W)$ [GeV]

- For more complicated processes and observables the phase space is extended but in less drastic ways.

- Add a parton to our previous example and demand one hard parton (jet) with a p_T above *20* GeV. Look at the *W* p_T distribution at the LHC.

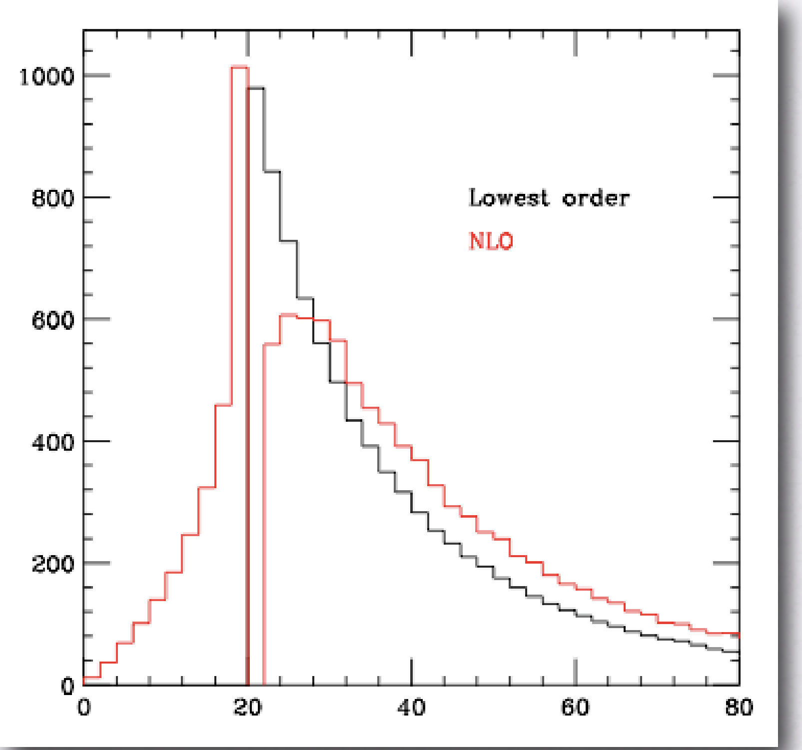

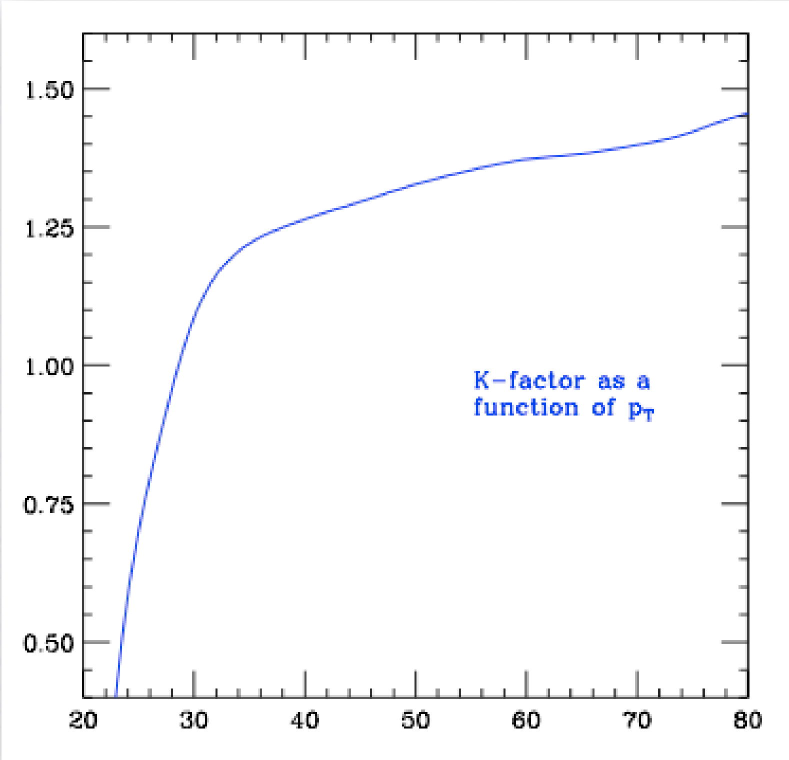

(K-factor strongly p_T-dependent)

- Just as before the *W* acquires a p_T by balancing the hard parton, which precludes the region below *20* GeV at LO. At NLO the real contribution contains events where the *W* balances against the vector sum of two partons with p_T(jet 1) and p_T(jet 2) > *20* GeV but $|\mathbf{p_T}(\text{jet 1})+\mathbf{p_T}(\text{jet 2})| < 20$ GeV.

- The alarming behaviour which occurs as the LO phase space boundary is approached indicates a large logarithm which should be resummed. It can also be “eliminated” by re-binning over a wide enough region.

- For processes which contain jets, the NLO corrections improve the lowest order picture in which each jet is modelled by a single parton.

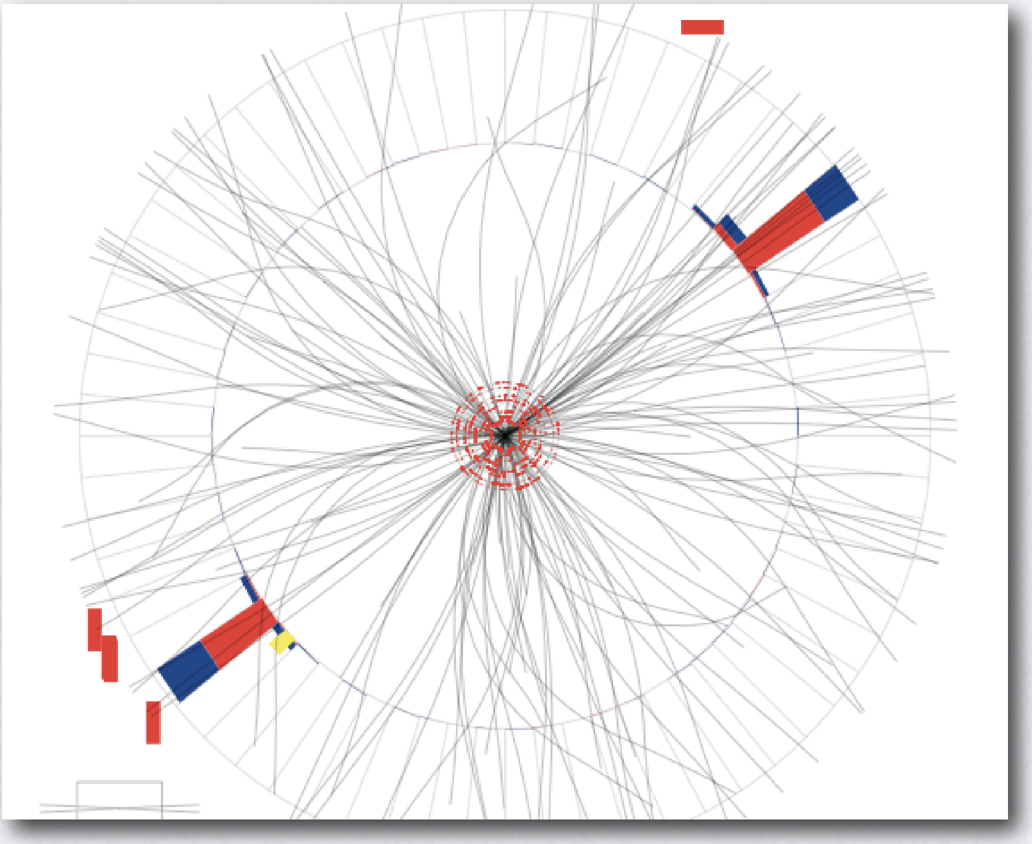

A jet event observed by D0

- In the detector a jet is the result of combining many tracks and has a definite size, for instance the radius of a cone in (η,φ) space.

- At NLO the same algorithm can be applied to try to combine two of the partons. The additional parton present in the real corrections can lie outside the original cone (and be observed as an additional jet) or inside it.

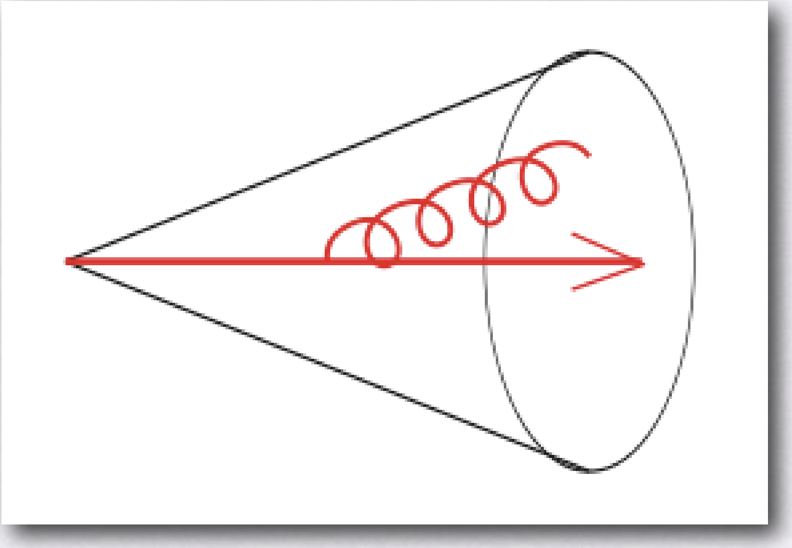

- Thus successive orders in α_s begin to build up a picture similar to that seen in the detectors, with multiple partons inside the jets.

- As a result, higher order calculations become sensitive to details of the jet-clustering algorithm - in particular, to how the partons are combined and to the size of the jet.

- *Scale-dependence* is the oft-cited reason for calculating higher-order QCD corrections.
- A perturbative calculation for a hadron collider involves the introduction of two scales.
  - The renormalization scale (μ_R) is needed in order to redefine bare fields in terms of physical ones. It is the scale at which the running coupling α_s is evaluated.
  - The factorization scale (μ_F) appears when absorbing the collinear divergences into the parton densities. One can think of this scale as separating the soft (non-perturbative) physics inside the protons from the hard process represented by the partonic matrix elements.
- By truncating the perturbative expansion at a given order, residual dependence on the chosen values of μ_R and μ_F remains.
- Often the scales are chosen to be equal and based on a hard scale that is present in the process, such as m_W or a minimum p_T. Any “reasonable value” is allowed though.
- Other strategies for choosing the scale are sometimes favoured, e.g. point around which scale dependence is smallest.

- A simple example is provided by the single-jet inclusive distribution at the Tevatron. At high E_T it is dominated by the quark-antiquark initial state.

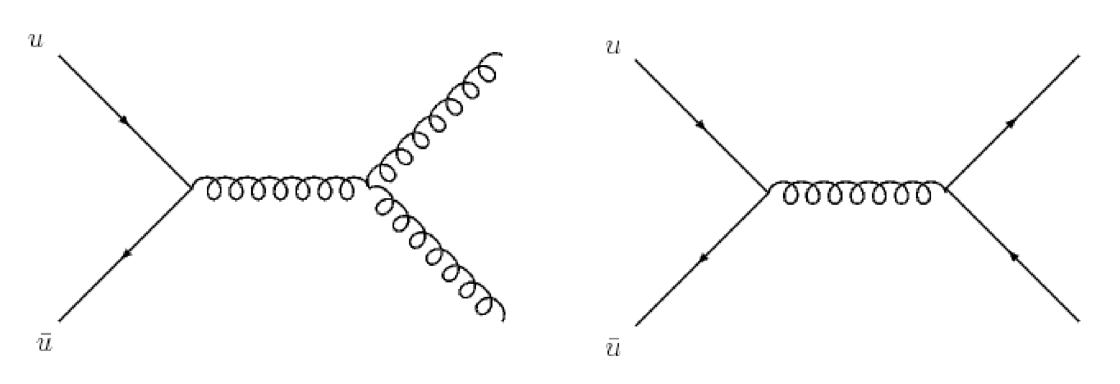

Glover, 2002

- At NLO the prediction can be written schematically as:

$$\frac{d\sigma}{dE_T} = \left[\alpha_s^2(\mu_R)\,\mathcal{A} + \alpha_s^3(\mu_R)\Big(\mathcal{B} + 2b_0\log(\mu_R/E_T)\,\mathcal{A} - 2P_{qq}\log(\mu_F/E_T)\,\mathcal{A}\Big)\right]$$

convolution with PDF

$$\otimes f_q(\mu_F) \otimes f_{\bar{q}}(\mu_F).$$

$b_0 = (33 - 2n_f)/6\pi$

Altarelli-Parisi splitting function from before

- In this expression, the explicit logarithms involving the renormalization and factorization scales have been exposed. The remainder of the α_s^3 corrections lie in the function *B*.

- Using the running of the coupling α_s and the DGLAP equation describing the evolution of the splitting functions,

$$\frac{\partial\alpha_s(\mu_R)}{\partial\log\mu_R} = -b_0\alpha_s^2(\mu_R) + \mathcal{O}(\alpha_s^3)\,, \qquad \frac{\partial f_i(\mu_F)}{\partial\log\mu_F} = \alpha_s(\mu_R)P_{qq}\otimes f_i(\mu_F) + \mathcal{O}(\alpha_s^2)$$

the NLO result is explicitly independent of μ_R and μ_F up to (unspecified) higher order terms.

Typical LO scale dependence

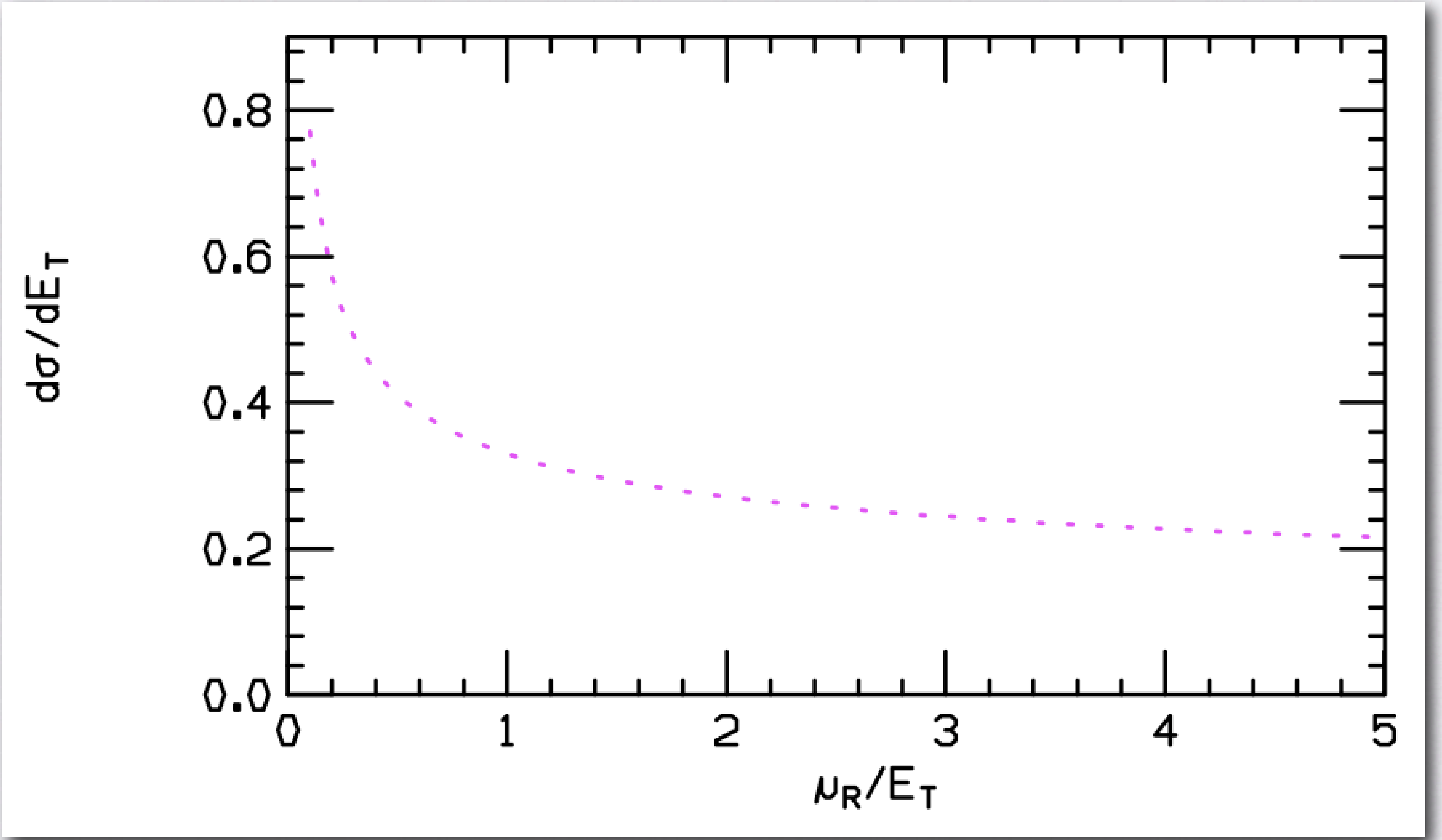

- The distribution at the Tevatron, for $E_T=100$ GeV. The factorization scale is kept fixed at $\mu_F = E_T$ and the ratio μ_R/E_T varied about a central value of *1*.
- At lowest order, the variation of the cross section just reflects the running of α_s. The prediction varies considerably as μ_R is changed so that the normalization of the cross section is unreliable.

Typical NLO scale dependence

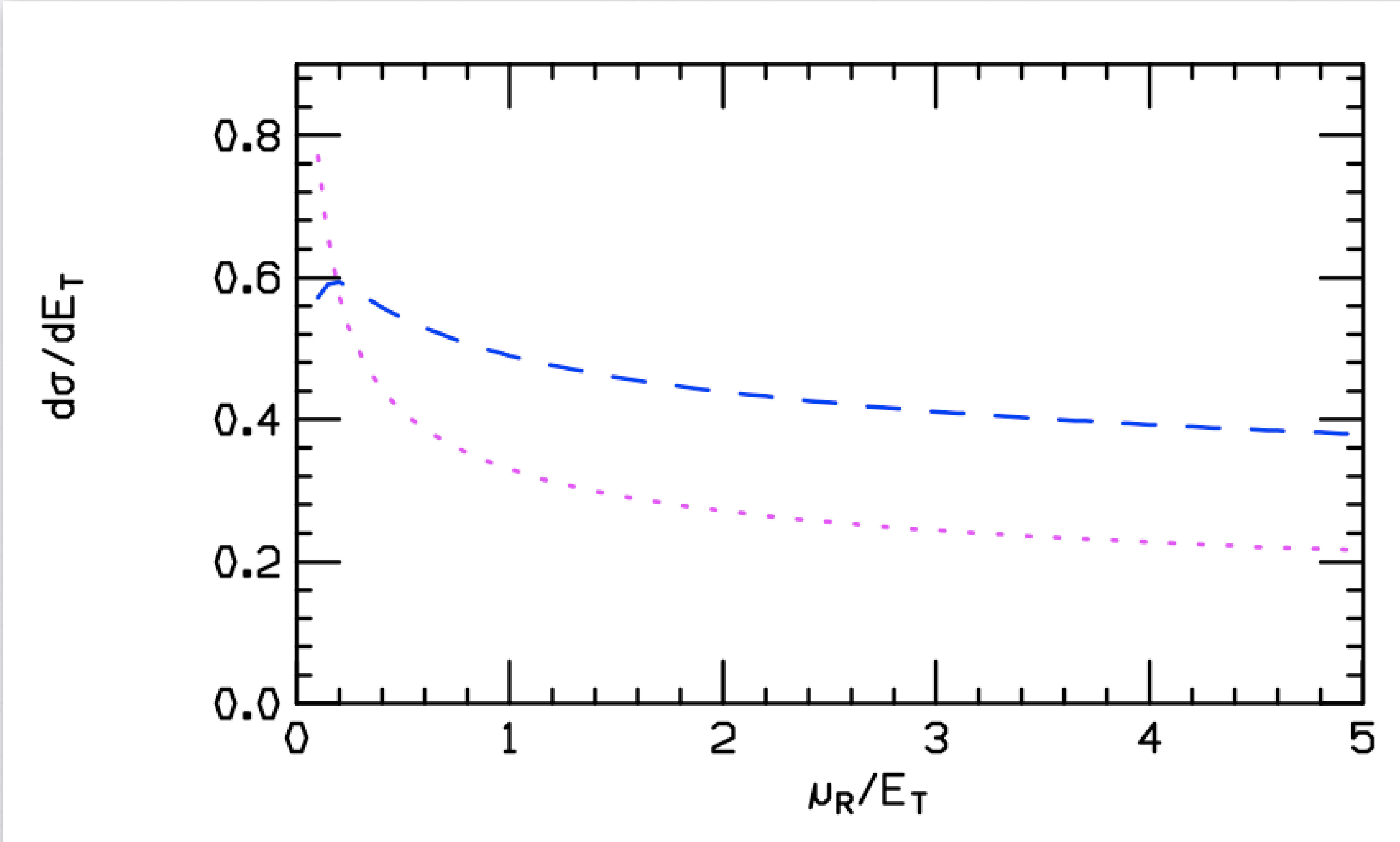

- At NLO, the growth as μ_R is decreased is softened by the logarithm that appears with coefficient α_s^3. The resulting turn-over is typical of a NLO calculation.
- As a result, the range of predicted values at NLO is much reduced and the first reliable normalization is obtained.

Typical NNLO scale dependence?

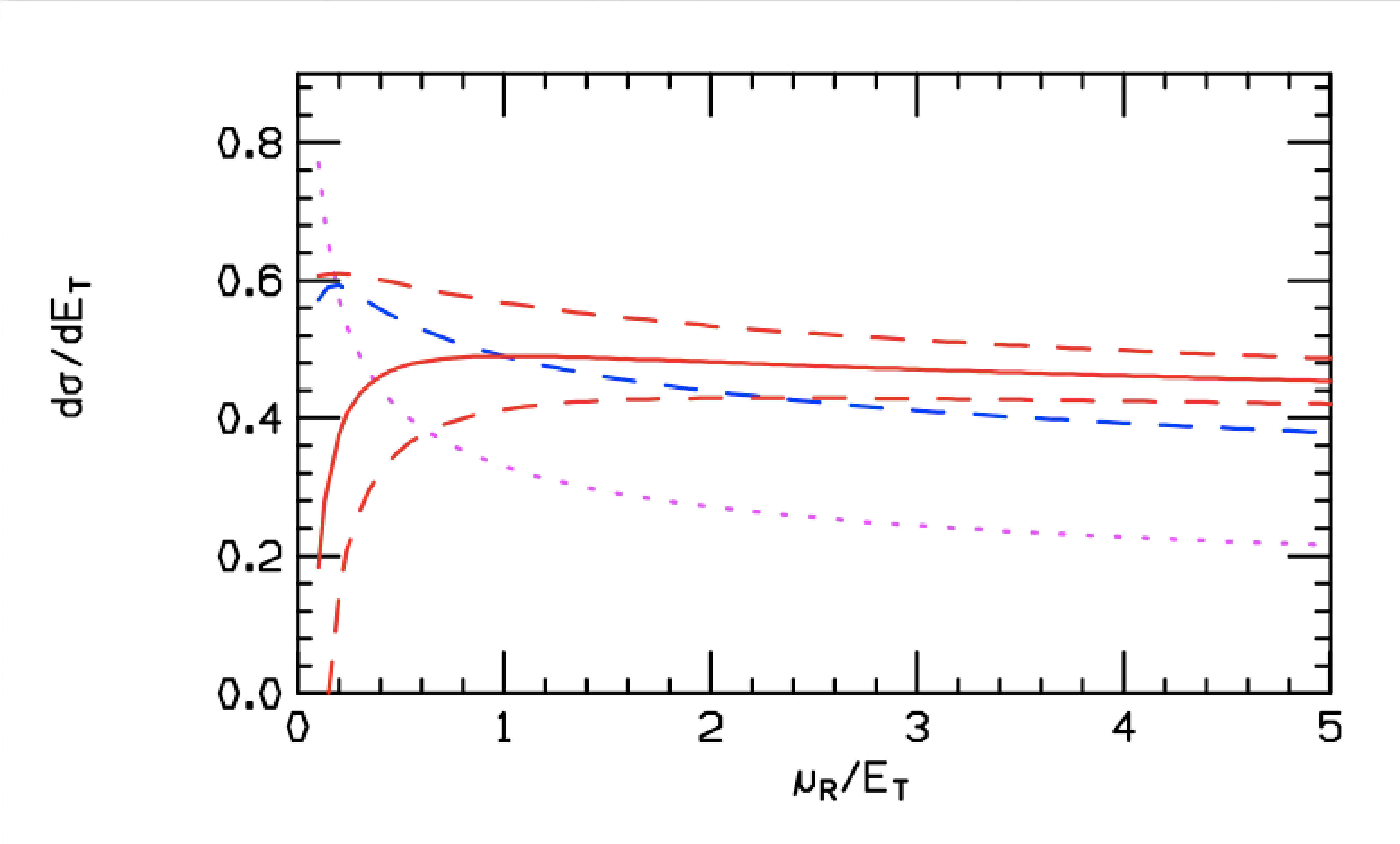

- The NNLO calculation for this process is not yet complete, but one can see the effect of reasonable guesses for the single unknown coefficient. We will return to this topic shortly.

- One therefore expects a theoretical error estimate of a few percent, which is the level required for many LHC analyses.

- However, this rosy picture is not always realized in every process.
- In particular, if the scale variation at LO is particularly small it is unlikely to be improved at NLO. This is especially apparent for purely electroweak processes which have no dependence on the renormalization scale at LO.

pp → *ZZZ* at the LHC   Lazopoulos & Melnikov, 2007

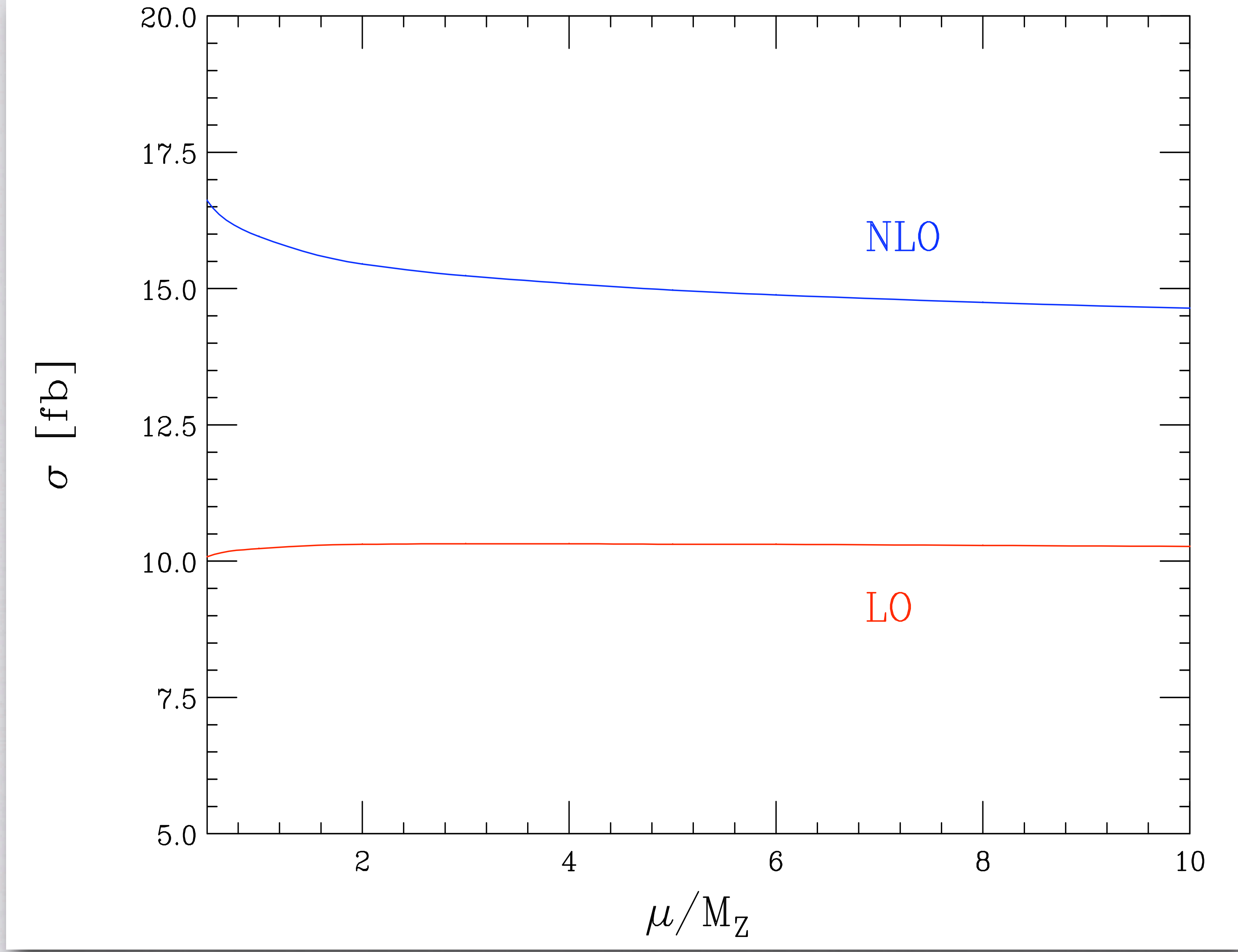

A recent pioneering calculation of this 2→3 scattering process

The loop integration is performed numerically. Singularities are extracted using *sector decomposition* and contours deformed to avoid internal thresholds.

Downside (in common with most other new approaches to NLO calculations): slow!

" ... ten thousand kinematic points required a few days of running on a cluster of several dozen processors."

- As well as the obvious real radiation diagrams obtained by radiating an additional parton in the final state, one must also include the corresponding crossed diagrams.

- These often introduce dependence of the cross section on new parton PDFs, e.g. our Drell-Yan calculation is insensitive to the gluon PDF at LO, but not so at NLO.

- The diagram contains a collinear singularity that is absorbed into the definition of the NLO PDF by subtracting a term proportional to P_{qg}.

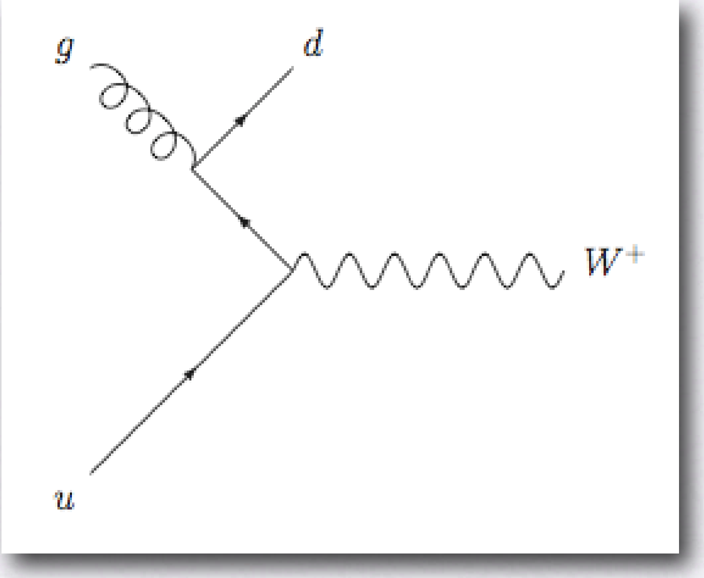

$g + u \to W + d$

- The inclusion of such contributions can have an important effect on the behaviour of the NLO cross section.

- In particular it can be the cause of worsened scale dependence, due to the fact that this NLO contribution depends on the scale in only a LO fashion.

- This is illustrated by the production of a *W* boson and two *b*-quarks at the LHC.

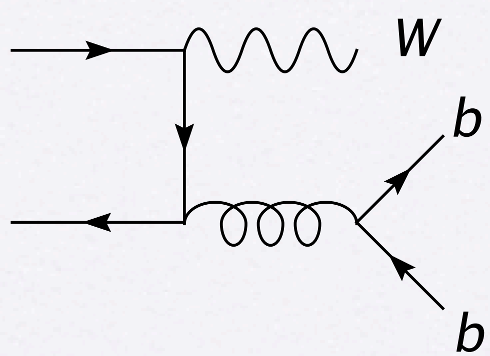

LO

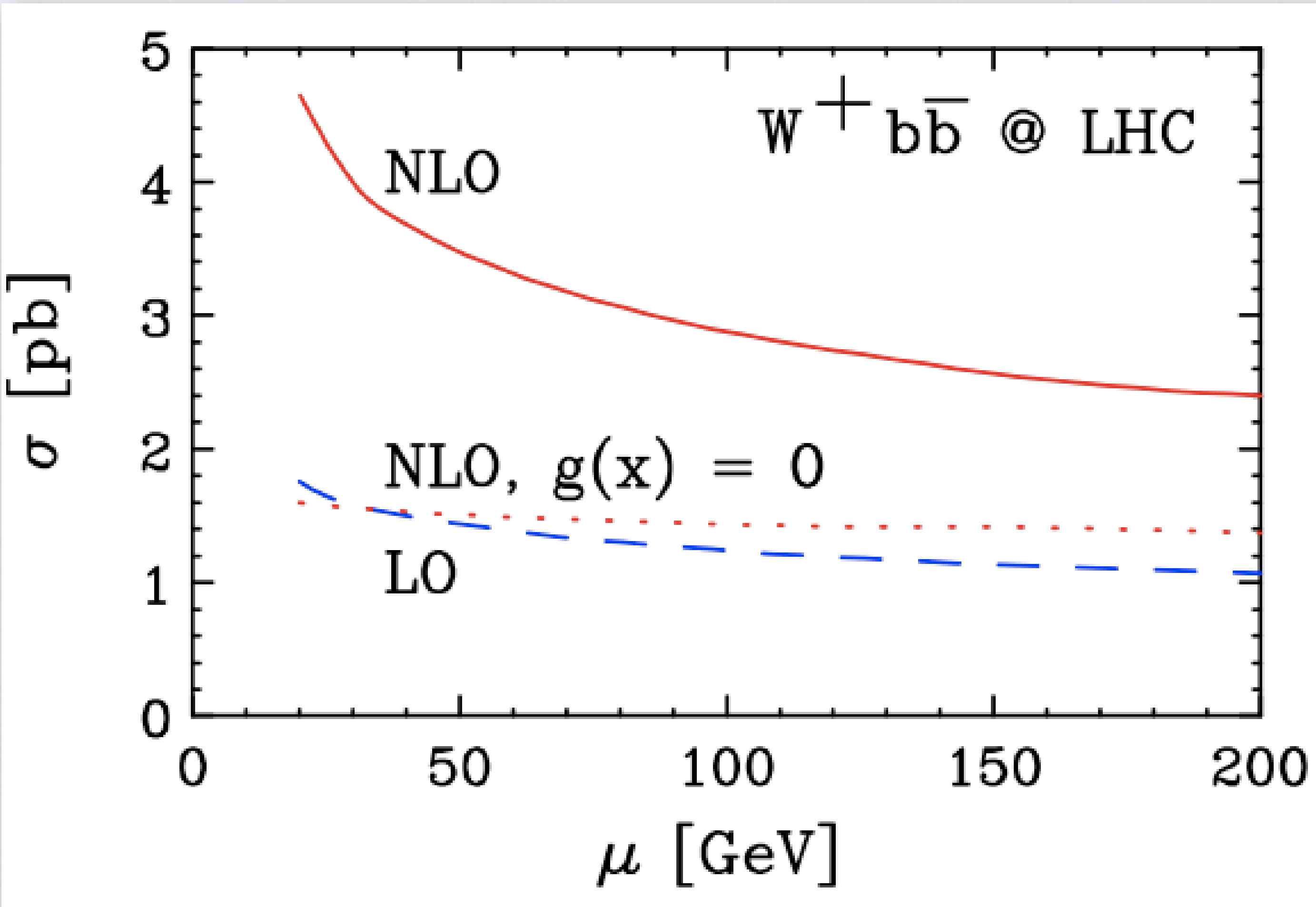

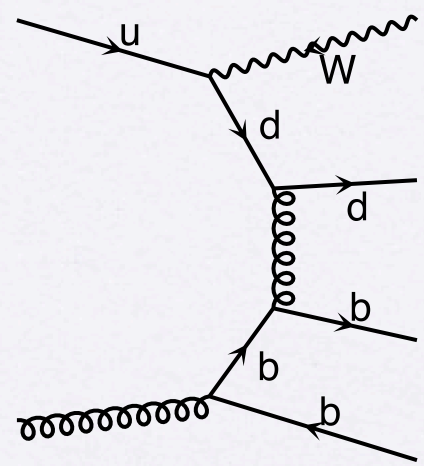

NLO

- Naively one would expect that $\sigma(Wbb\text{+jet}) < \sigma(Wbb)$, but this is not the case (for this definition of a jet, $p_T > 20$ GeV) because of the high gluon flux at the LHC. The *Wbb* final state is very likely to be accompanied by additional hadronic activity at the *20* GeV level.

- It is a warning sign that the LO cross section may not be the basic process of interest in this case.

- A similar situation regarding the additional radiation occurs in top quark production.

- At the Tevatron, where typical jet transverse momenta are of the order of *10-20* GeV the situation looks fine.

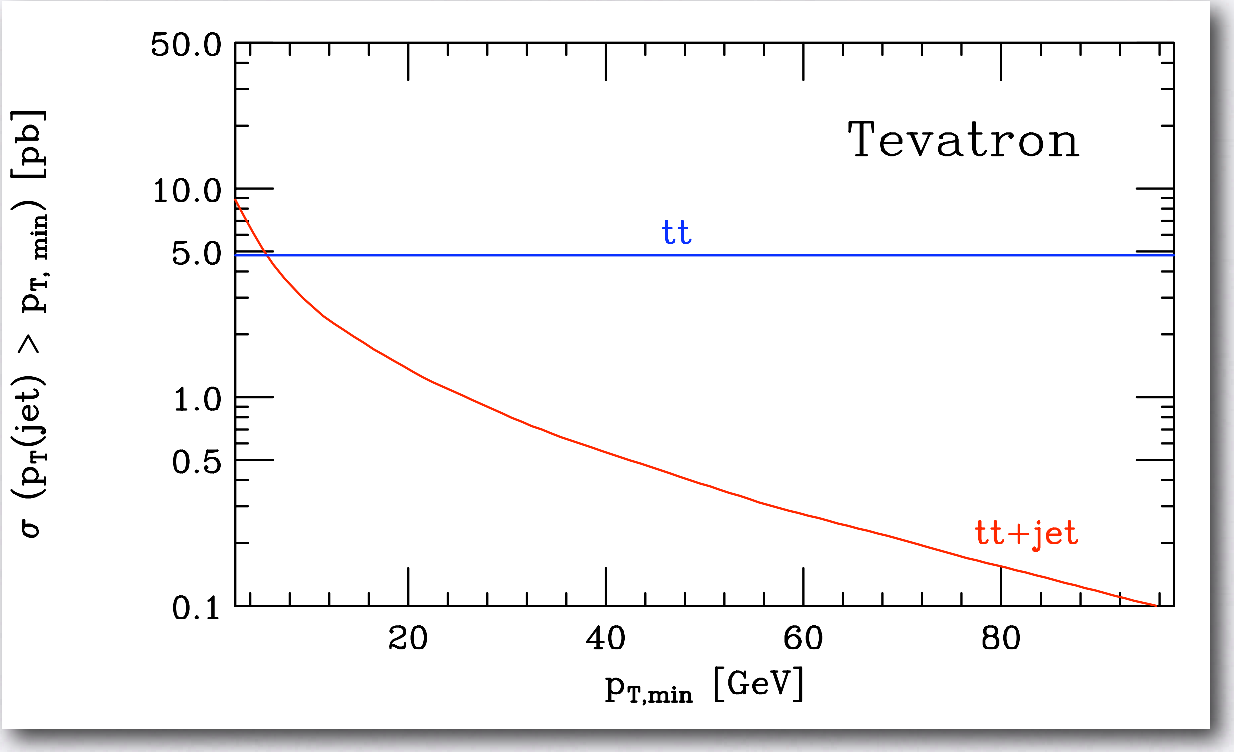

- At the LHC it is not so clear. Perhaps we'll just need to adjust our definition of a jet.

- This phenomenon is not unusual. The same behaviour occurs, for example, in Higgs production via gluon fusion.

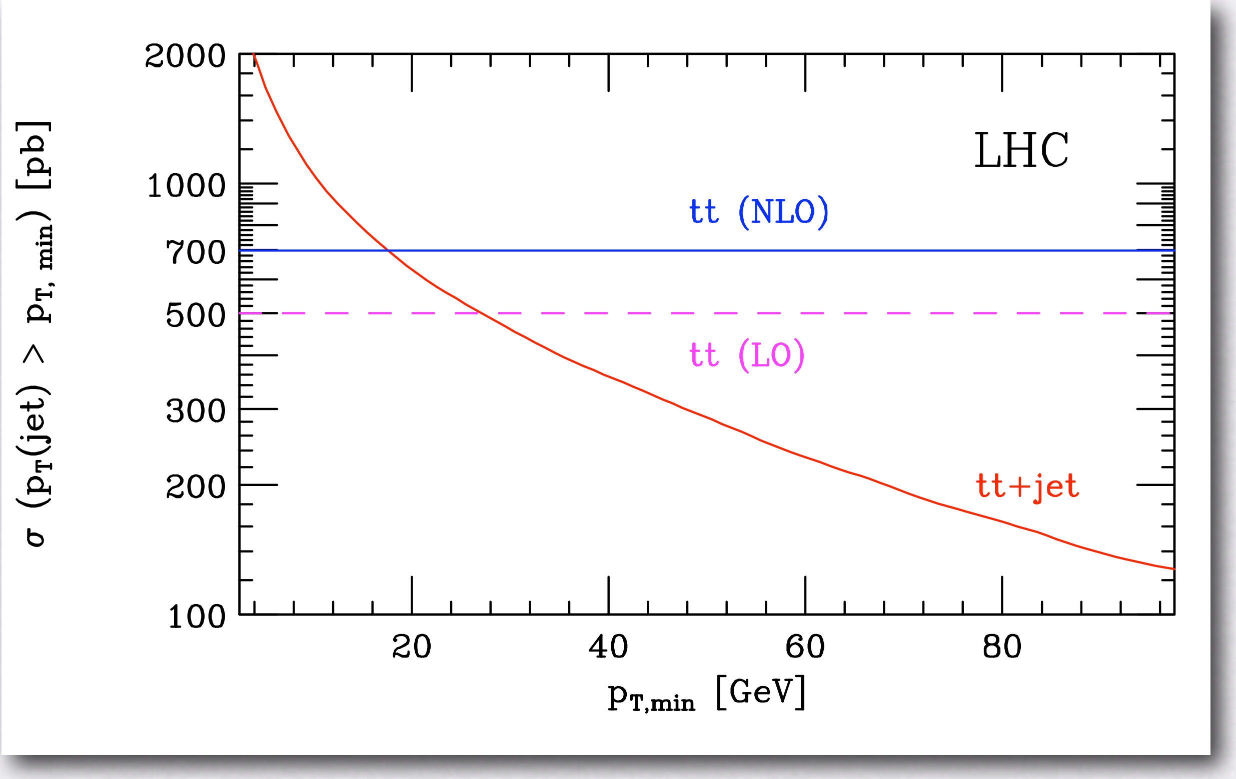

- The NLO calculation of the top pair + jet process has very recently been completed.

  Dittmaier, Uwer & Weinzierl, 2007

- Due to the presence of pentagon loop integrals with an internal mass, this is one of the most complex NLO calculations performed so far.

- The results show that this process exhibits canonical scale dependence and that the corrections are not terribly large, for the usual scale choices.

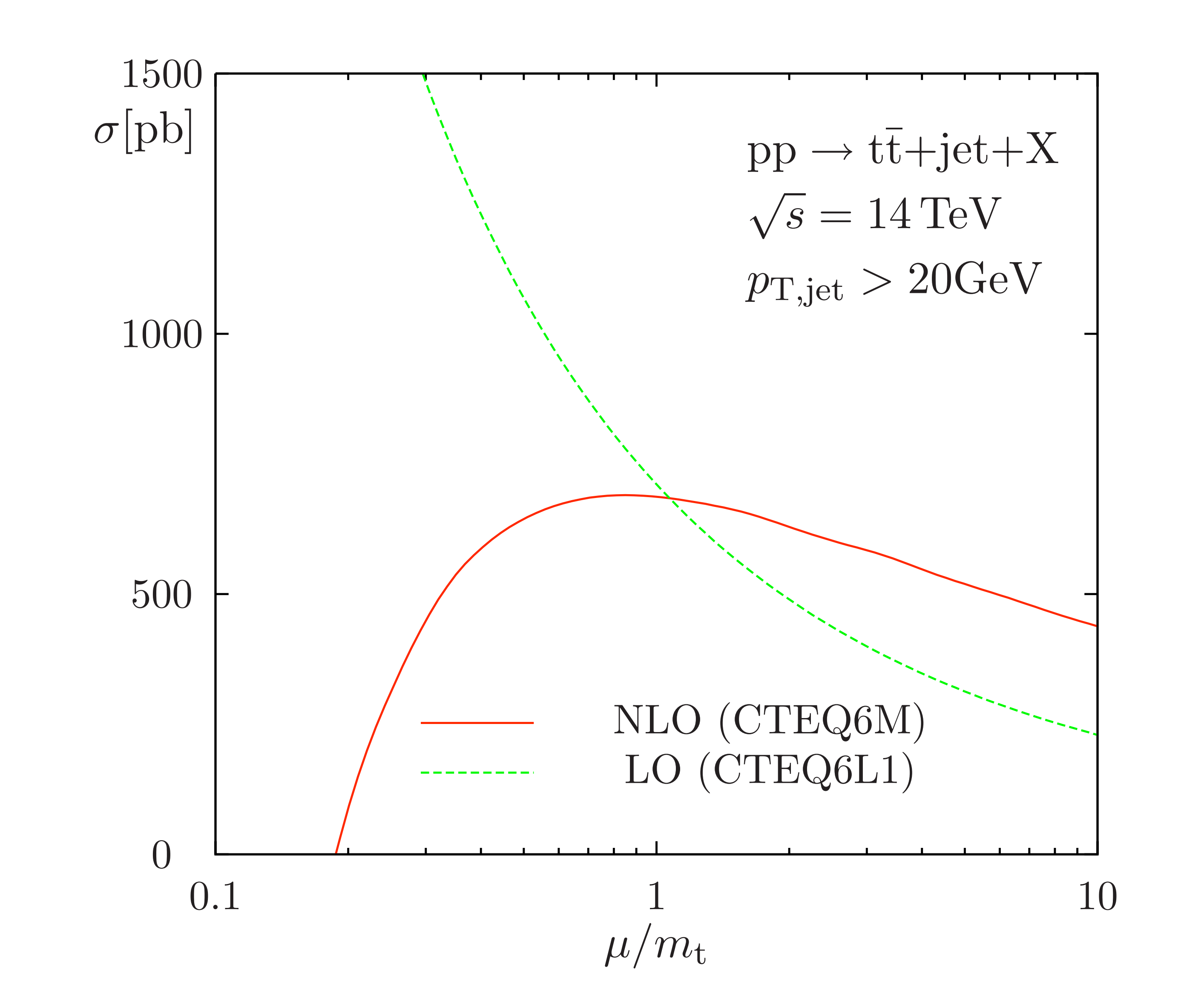

Summary of NLO advantages

- It can provide a more accurate normalization of the cross section which is in general larger than the LO prediction.
  - However this is not always the case, particularly in kinematic regions where the prediction is essentially LO.
  - When the scale dependence is not much improved (or worse) than at LO, we must either reconsider the physics process in which we are interested or consider moving to higher orders in PT.
- It begins to include the effects of radiation that are especially important when comparing with jet data.
- The phase space available to observables is often extended at NLO, enabling comparison with a wider range of experimental data.
- Whilst large corrections can indicate problems with the perturbative approach, they help identify regions in which a large logarithm exists and can be resummed. By matching such a calculation with NLO an even more powerful prediction is obtained.

- e.g. for top production at the Tevatron, the NLO corrections are large in the threshold region.
- These are due to soft gluon radiation which, as we've seen, leads to logarithms which can be identified predictably. They can then be exponentiated and resummed to all orders.

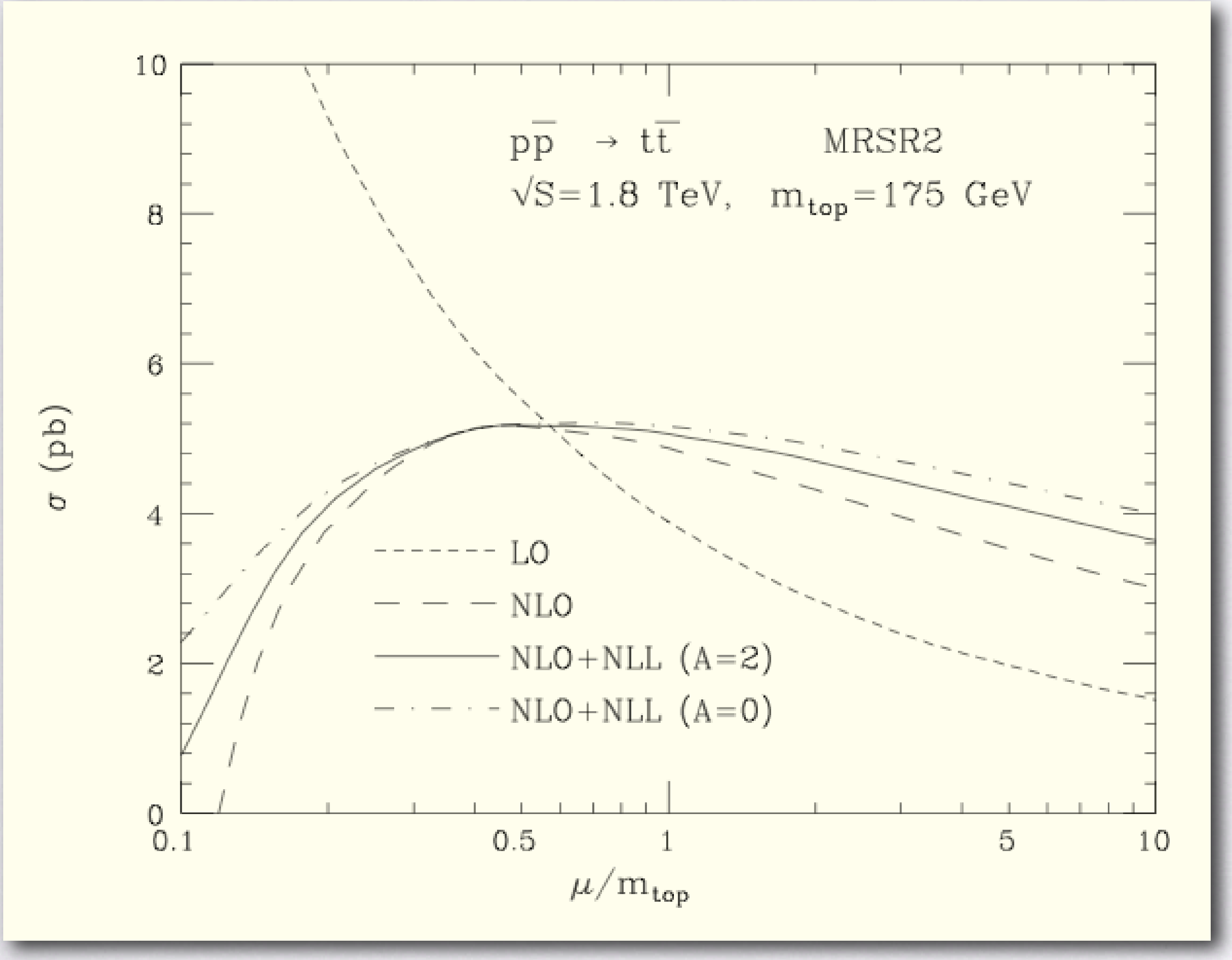

Bonciani, Catani, Mangano, Nason, 1998

scale uncertainty reduced from 10% to 5% by improving NLO to include NLL

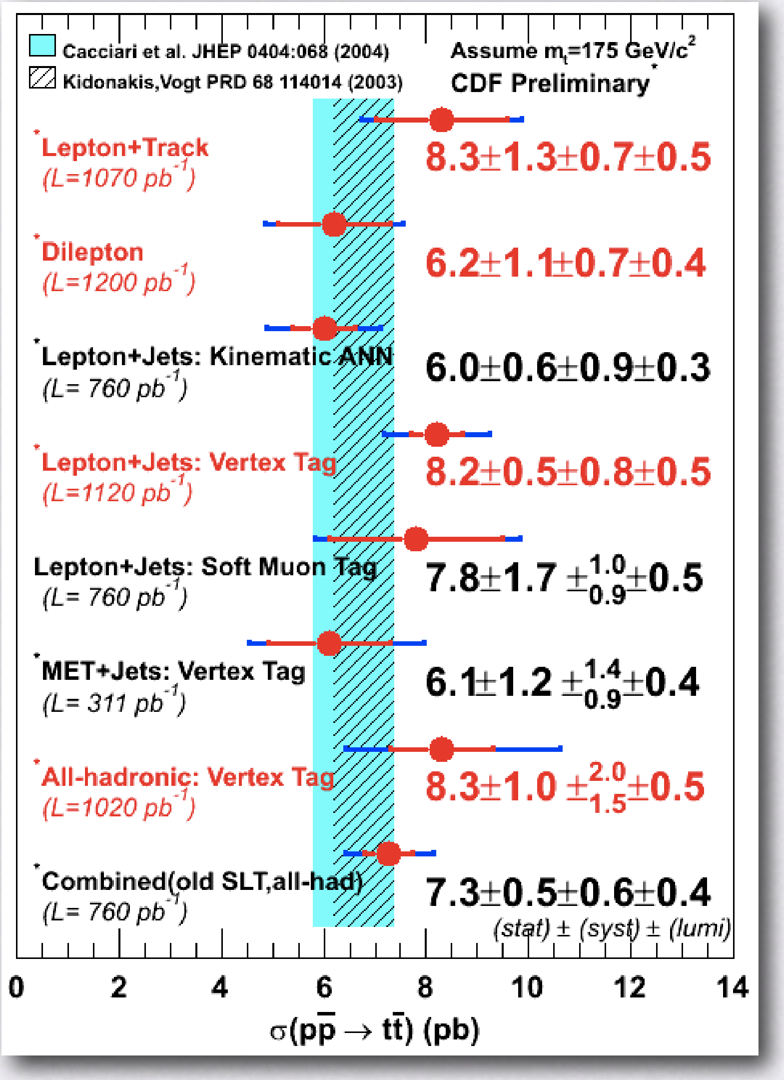

- Clearly, NLO alone is not always enough.
- Apart from combining with a formal resummed calculation, another (highly desirable) approach is to include NLO information in a *parton shower.*
- As you have heard already from F. Krauss, such procedures are well underway and some have been available for a few years already.
- The most widespread example is *MC@NLO* which provides a NLO parton shower for a small number of relatively simple processes (but that number is steadily growing).

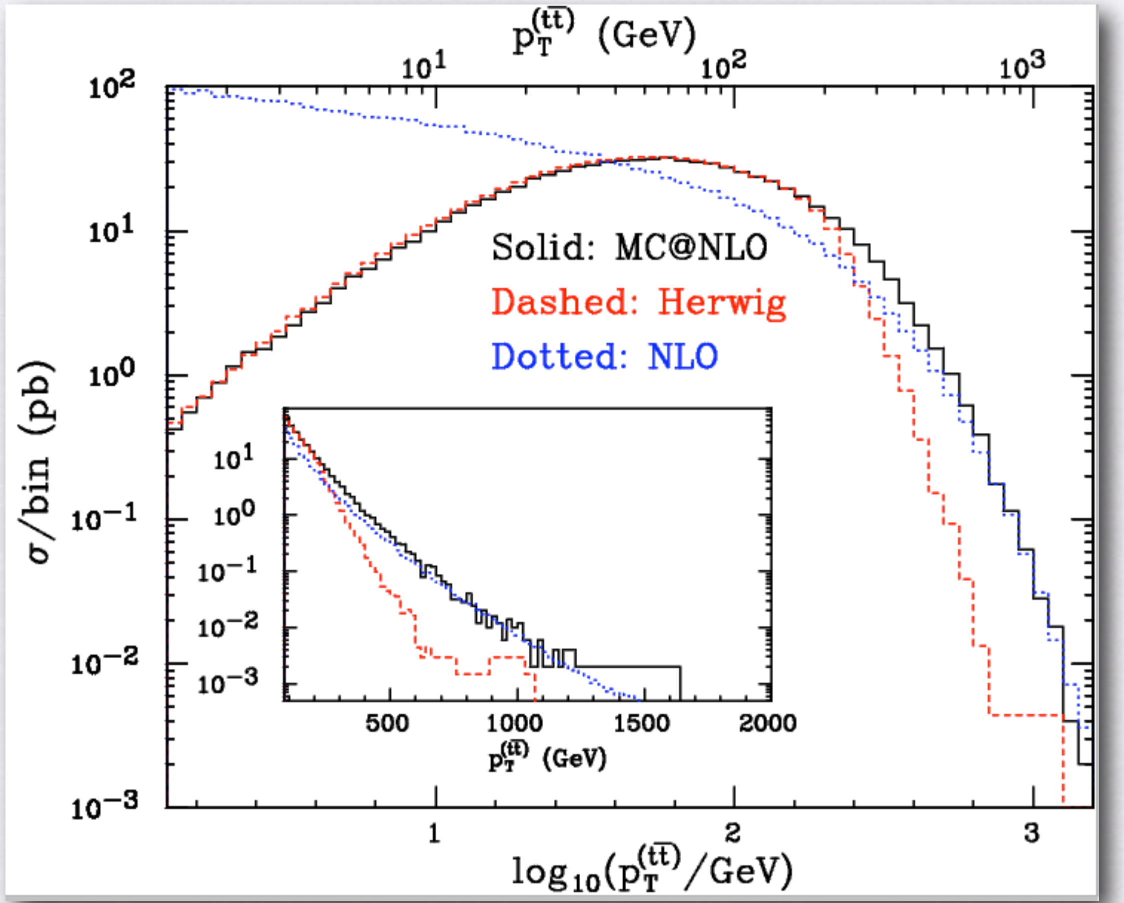

The prediction retains the best characteristics of both worlds.

It contains information on the NLO normalization and scale dependence, together with the good infrared behaviour of the shower (and everything else).

Frixione and Webber, 2003

NLO wishlist

- Despite some obvious shortcomings, the calculation of NLO corrections remains a high priority, particularly to aid the LHC experiments in the early years when data-driven analyses are not yet possible.
- Indeed, some extravagant wishlists of backgrounds that one would like to know at NLO have been concocted over the years.
- Limited manpower means we have to prioritize by necessity and feasibility.

process $(V \in \{Z, W, \gamma\})$	relevant for
1. $pp \to V\,V$+jet	$t\bar{t}H$, new physics
☑ $pp \to H + 2$ jets	H production by vector boson fusion (VBF)
3. $pp \to t\bar{t}\,b\bar{b}$	$t\bar{t}H$
☑ $pp \to t\bar{t} + \cancel{2}$ 1 jets	$t\bar{t}H$
5. $pp \to V\,V\,b\bar{b}$	VBF$\to H \to VV$, $t\bar{t}H$, new physics
6. $pp \to V\,V + 2$ jets	VBF$\to H \to VV$
7. $pp \to V + 3$ jets	various new physics signatures
☑ $pp \to \cancel{V\,V\,V}$ ZZZ	SUSY trilepton searches

Les Houches workshop, 2005

Dominated by final states containing b-quarks, high p_T leptons and missing energy.

All are either *2*→*3* processes (*3* done so far!) or *2*→*4* (still just a dream ...).

- So far there have been many implementations of NLO matrix elements for *2*→*1*, *2*→*2* and some *2*→*3* processes, scattered across multiple codes.

- As another shameless plug, I'll briefly mention my own work on NLO corrections, most of which is included in the package MCFM.

J.C., K. Ellis
(+ F. Tramontano,
F. Maltoni,
S. Willenbrock)

http://mcfm.fnal.gov/

$p\bar{p} \to W^\pm/Z$	$p\bar{p} \to W^+ + W^-$
$p\bar{p} \to W^\pm + Z$	$p\bar{p} \to Z + Z$
$p\bar{p} \to W^\pm + \gamma$	$p\bar{p} \to W^\pm/Z + H$
$p\bar{p} \to W^\pm + g^\star\,(\to b\bar{b})$	$p\bar{p} \to Zb\bar{b}$
$p\bar{p} \to Zb$	$p\bar{p} \to Wb$
$p\bar{p} \to Zbj$	$p\bar{p} \to Wbj$
$p\bar{p} \to W^\pm/Z + 1$ jet	$p\bar{p} \to W^\pm/Z + 2$ jets
$p\bar{p}(gg) \to H$	$p\bar{p}(gg) \to H + 1$ jet
$p\bar{p}(VV) \to H + 2$ jets	$p\bar{p} \to t\bar{t}$
$p\bar{p} \to tX$ (t and s-channel)	$p\bar{p} \to t + W$
$p\bar{p}(gg) \to H + 3$ jets,(LO)	$p\bar{p} \to t\bar{t}g$,(LO)

- The package includes a number of NLO calculations in one place.

- The flagship processes are *W/Z+2* jets and *H+2* jets via gluon fusion (not yet available publicly - it is slow and somewhat cumbersome compared to the other calculations that are already included).

$$A = \frac{g^2}{12\pi^2 v}$$

$$\mathcal{L}_{\rm eff} = \frac{1}{4} A(1+\Delta) H G^a_{\mu\nu} G^{a\,\mu\nu}$$

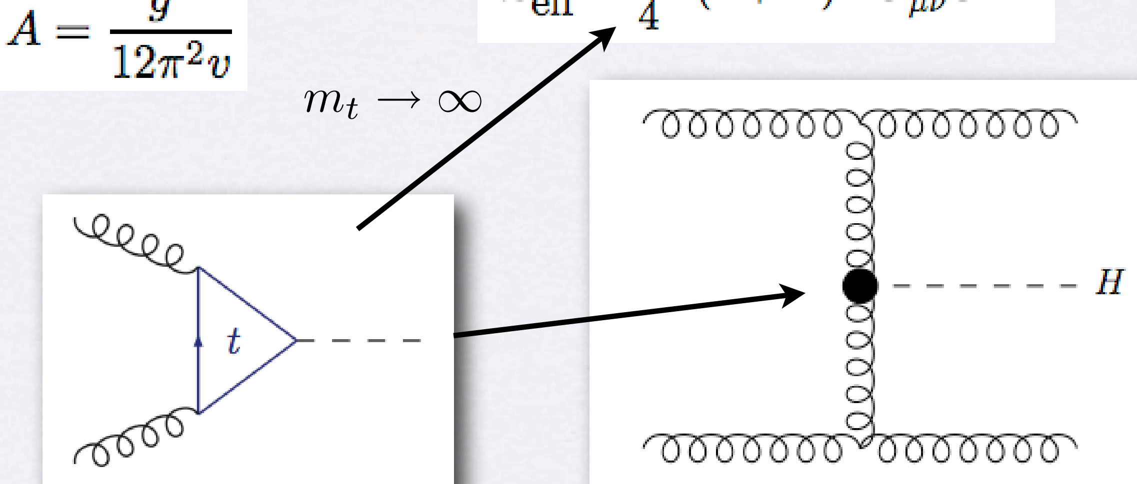

- However, to tackle some of the processes on the wishlist, it is clear that new methods for performing the calculations are needed.

- Recent *twistor-inspired* advances have already provided ground-breaking results for some of the 1-loop amplitudes - see the lectures by R. Roiban.

- Another approach which has provided both a useful cross-check of these results and a full (parton-level) MC implementation is semi-numerical.

Ellis, Giele and Zanderighi, 2005

- In this approach, the tensor integrals are reduced to a set of master integrals in an algorithmic fashion similar to Passarino-Veltman reduction.

- However, at each stage the reduction is performed numerically. Only the final set of master integrals is implemented analytically.

- Clearly, great care must be taken to ensure that the reduction is numerically stable across phase space.

- This procedure is also computationally expensive; nevertheless this is the method used for the calculation of H+2 jet production in MCFM.

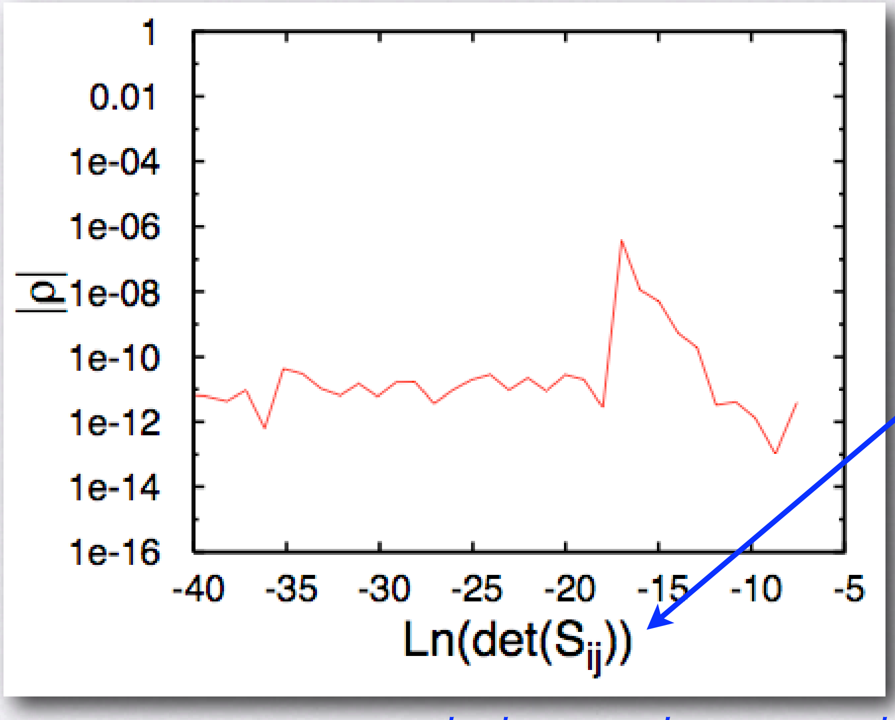

comparison with the simplest 4-quark amplitude (calculable analytically)

Higher orders still

- The other obvious direction is to move to the next higher order, NNLO.
- We've already seen how the scale dependence is expected to be reduced even further.
  - Just as we might begin to trust the normalization of a cross section at NLO, the theoretical uncertainty associated with it is only reasonably estimated at NNLO.
- In addition, many of the arguments for NLO apply again at NNLO - e.g. even more sensitivity to jet algorithms, still larger phase space, etc.
- The ingredients for a NNLO calculation are similar to, but more complicated than, those that enter at NLO.
- They can be viewed by considering all possible cuts of a 3-loop diagram.
- A lot of recent effort has been focused on the calculation of the 3-jet rate in e^+e^- annihilation.

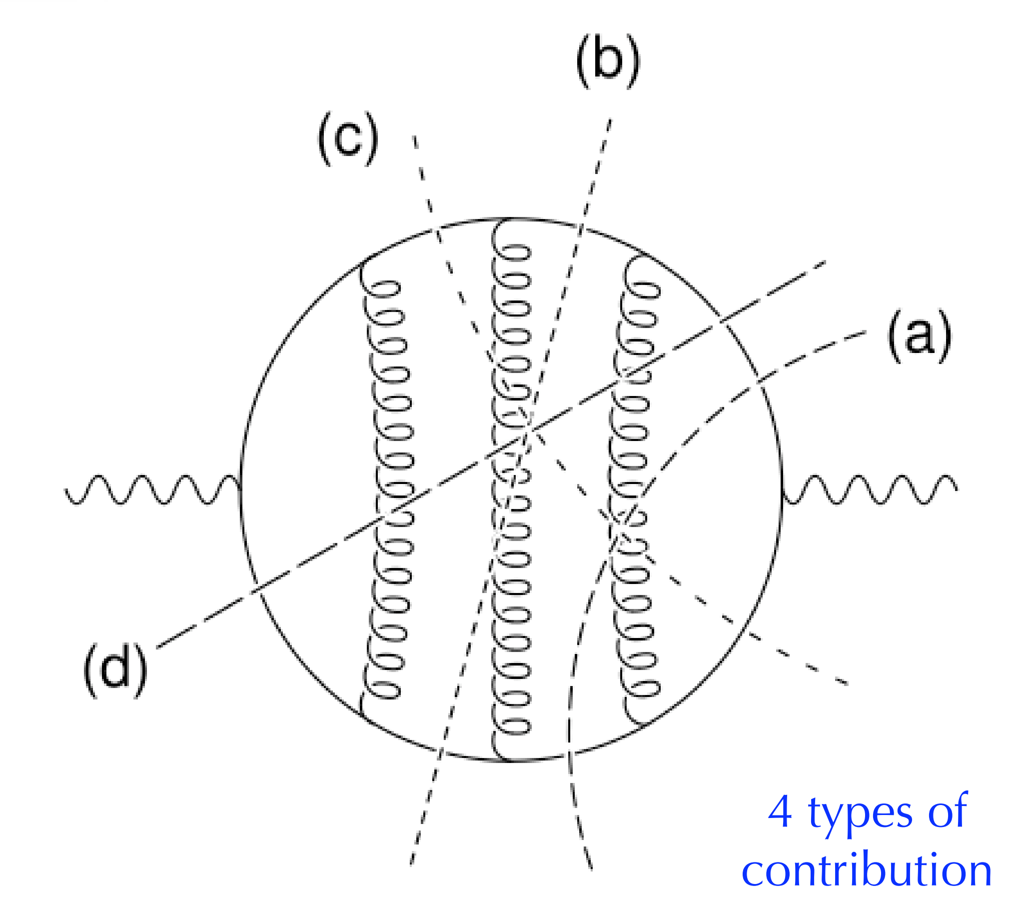

- The most obvious contribution is the cut which represents the interference of 2-loop diagrams with LO.
- As the result of much innovative work over the last 10 years, this contribution is now known.
- This included deriving all the necessary master integrals, as well as formulating the tensor decomposition in terms of them.

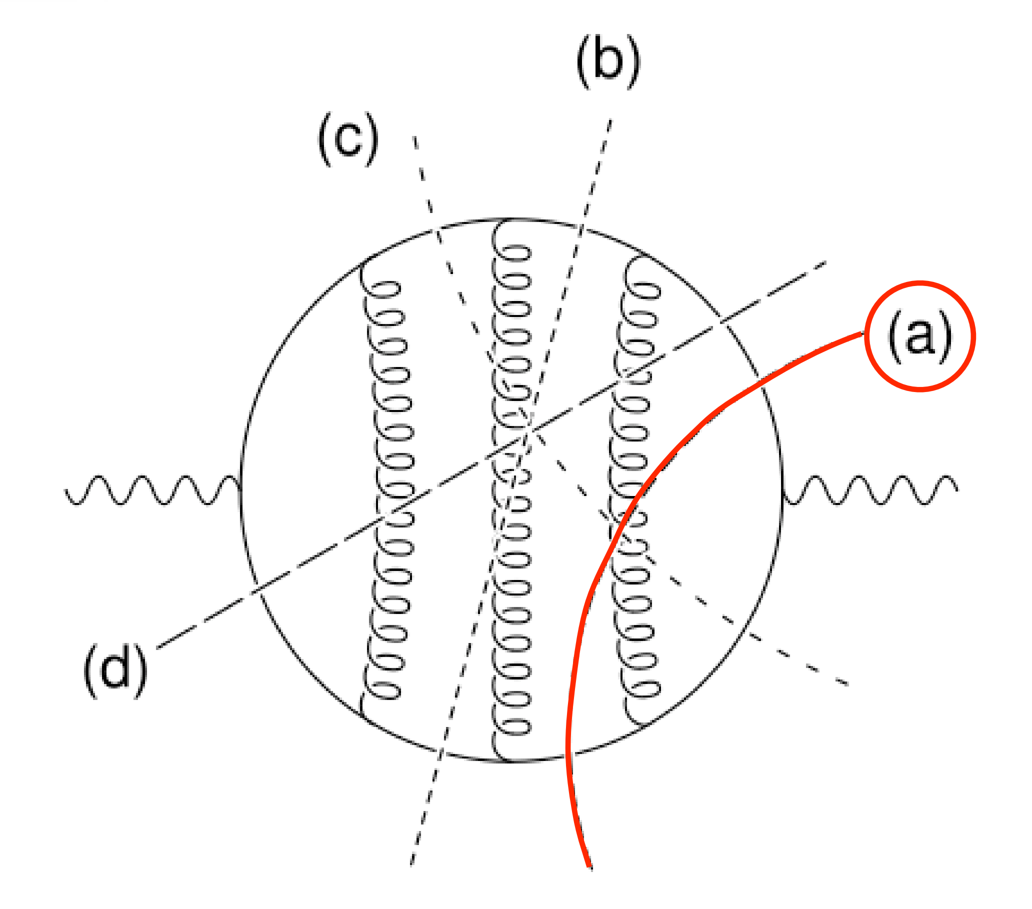

- By using similar methods, and using crossing symmetries, a number of 2-loop matrix elements relevant for hadron colliders are now known.
  - Drell-Yan, Higgs production (via gluon fusion and associated with a *W/Z*)
  - dijet, diphoton production
  - production of a vector boson and a single jet

A large army of 2-loop stalwarts, see for example a recent talk by Gehrmann, hep-ph/0709.0351

- The multiplicity of particles in the final state is very small, due to the complexity of the loop integrals.

- The second contribution is the square of the 1-loop amplitudes that already entered the NLO calculation (but as an interference).

- They are therefore straightforward to obtain in general. However, sometimes the NLO calculation will have calculated the interference with the LO amplitude only, so they might not be directly available.

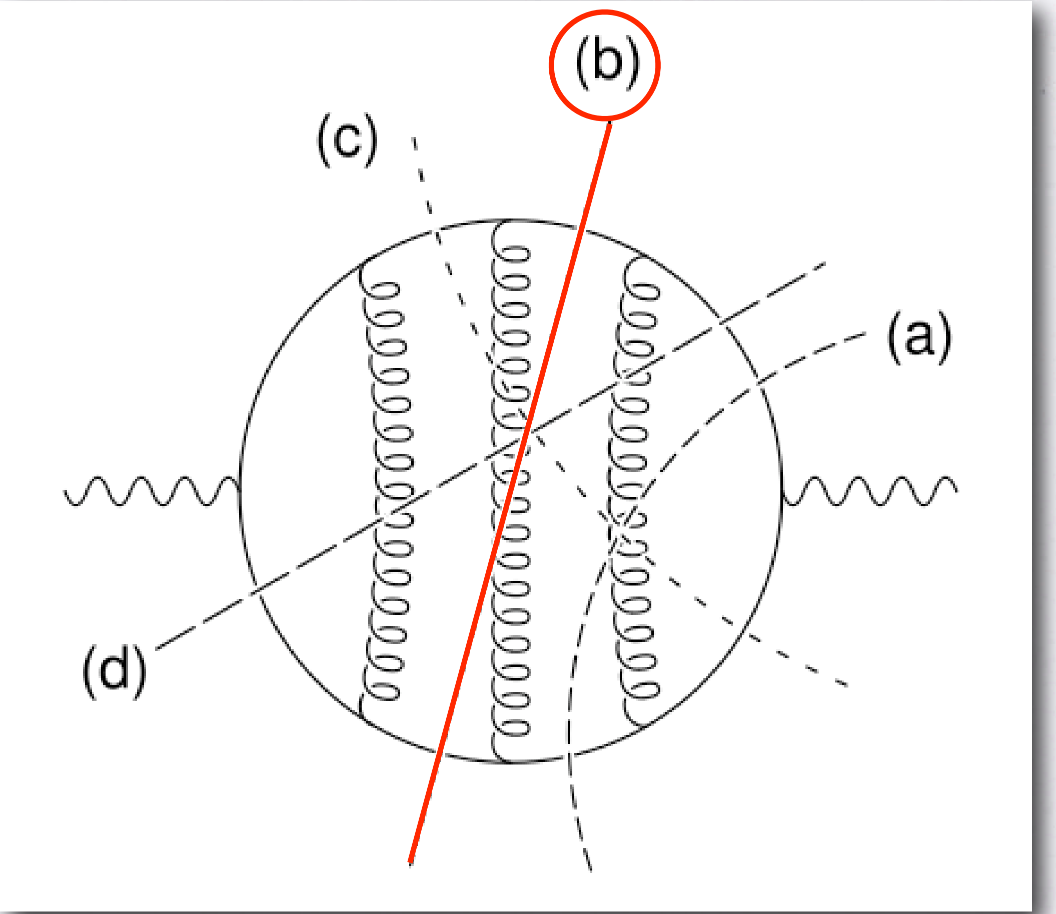

- The third cut reveals an interference between the LO and 1-loop amplitudes with 4 partons.

- Just as in the real contributions at NLO, this contains divergences when two of the partons are unresolved.

- Methods to extract all the singularities are by now well-known.

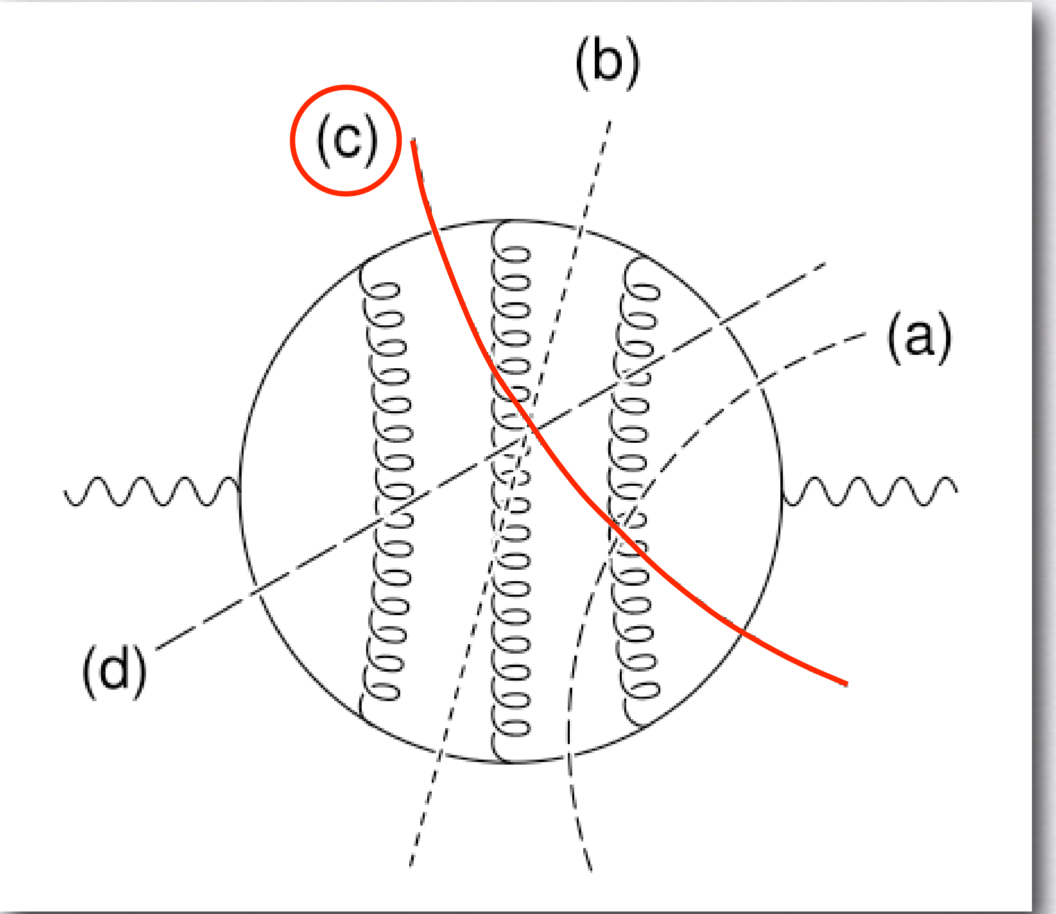

- The final contribution looks deceptively simple - it is just LO matrix elements squared.

- However, it contains singularities when two of the partons cannot be resolved from the others.

- The singular configurations can be divided into four categories:
  triply collinear *doubly collinear*
  doubly soft *soft-collinear*

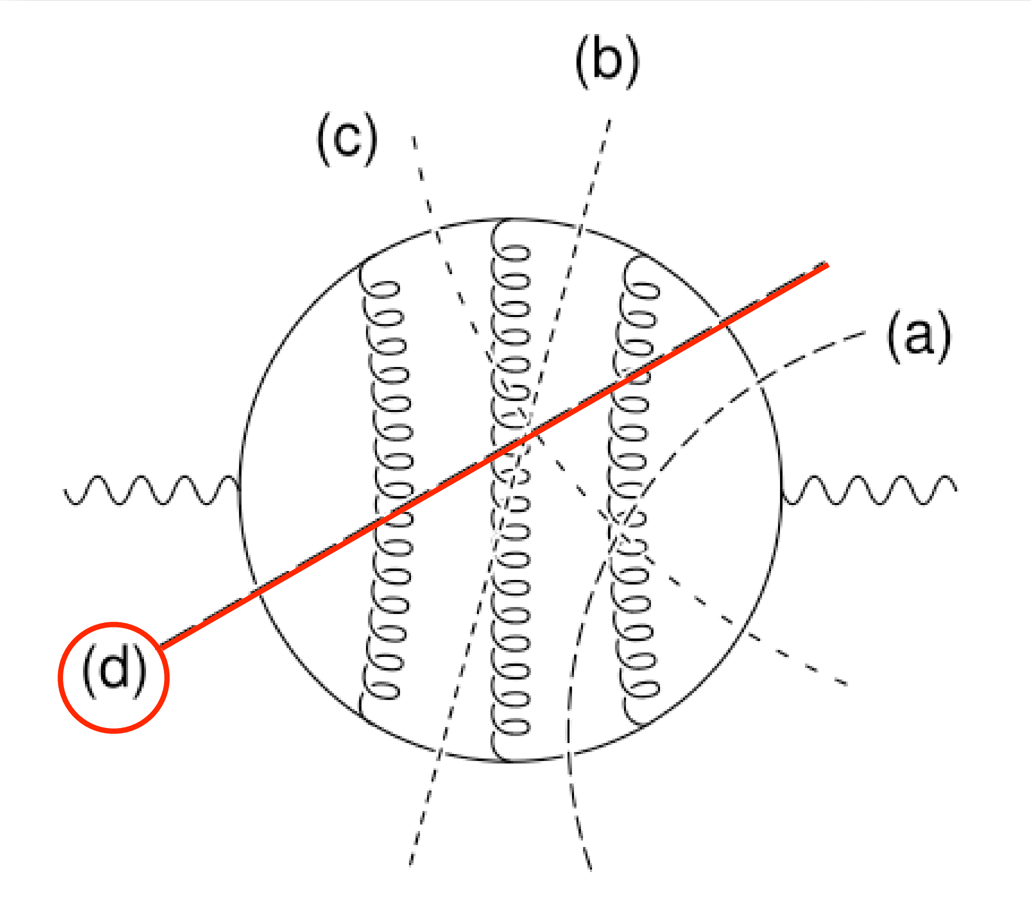

- As we discussed, at NLO the equivalent singular regions are handled in a systematic fashion using the technique of PS slicing or subtraction.

- For a long time, the extension of such a general method to NNLO was not available. A few calculations were performed using special tricks and on a case-by-case basis.

- The *antenna-subtraction method*, not dissimilar to dipole subtraction at NLO, encodes all singular behaviour between a colour-connected pair of hard partons. This method has been successfully applied at NNLO.
  Gehrmann-de Ridder, Gehrmann, Glover, 2005.

- Much of the hard work lies in performing the analytic integrals over the singular region of phase space to extract the poles in ϵ.

- First results using this method have only very recently been presented.
  Gehrmann-de Ridder, Gehrmann, Glover, Heinrich, 2007.

$$
\begin{aligned}
d\sigma_{NNLO} = & \int_{d\Phi_5} \left(d\sigma^{R}_{NNLO} \overset{(d)}{} - d\sigma^{S}_{NNLO} \right) \\
& + \int_{d\Phi_4} \left(d\sigma^{V,1}_{NNLO} \overset{(c)}{} - d\sigma^{VS,1}_{NNLO} \right) \\
& + \int_{d\Phi_5} d\sigma^{S}_{NNLO} + \int_{d\Phi_4} d\sigma^{VS,1}_{NNLO} + \int_{d\Phi_3} d\sigma^{V,2}_{NNLO} \overset{(a),(b)}{}
\end{aligned}
$$

each line is separately finite and can be integrated numerically

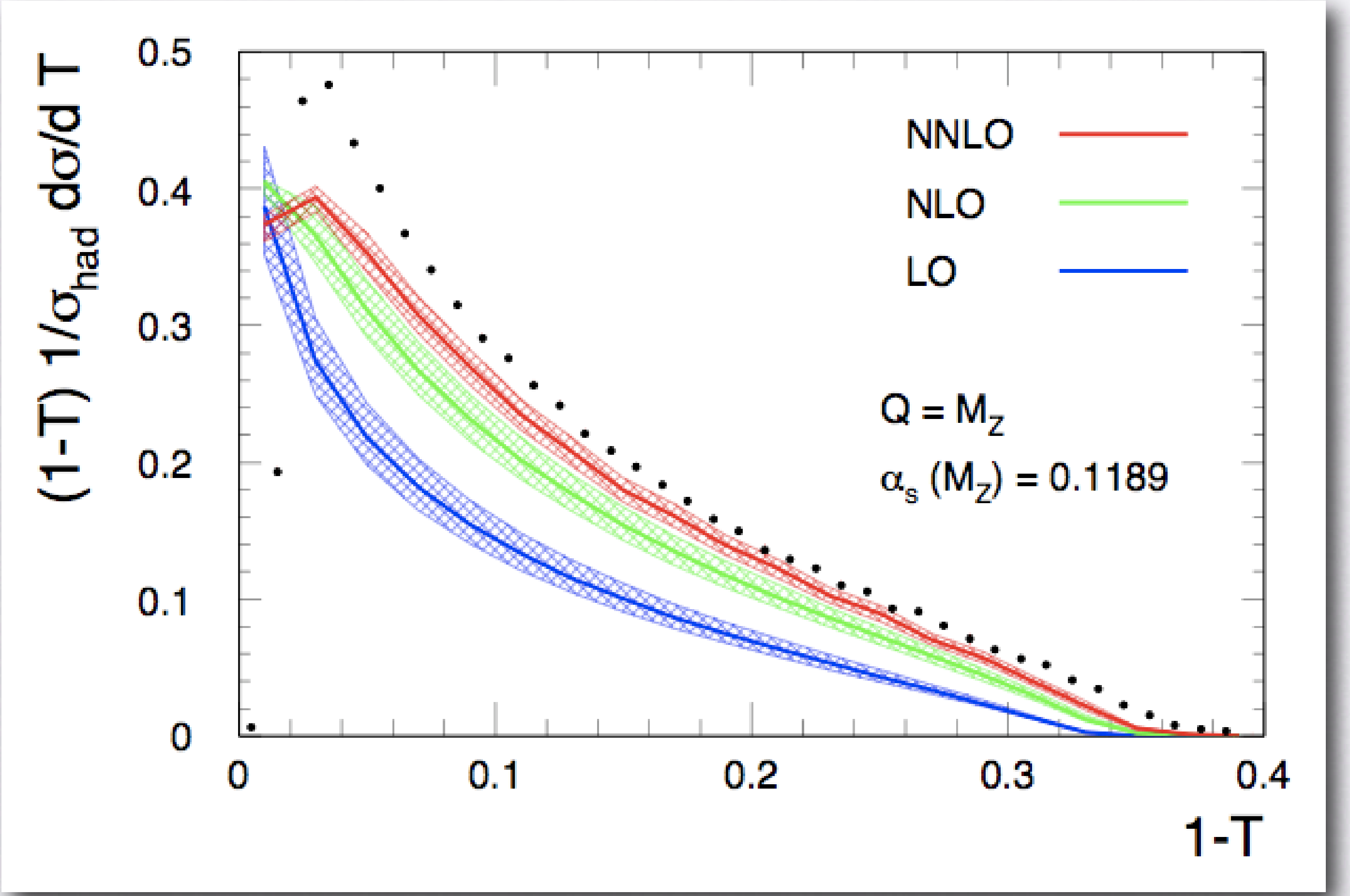

Thrust distribution at LEP

Modest increase in prediction and reduction in scale uncertainty when going from NLO to NNLO

Improvement in shape when compared with ALEPH data (dots), requiring smaller hadronization corrections

- The prognosis for adapting this calculation to hadron colliders is good, although undoubtedly some technical issues remain.
- For now we must be content with more inclusive calculations for *2→1* processes, such as *W/Z/H* production.
- The NNLO prediction can be computed differentially in the boson rapidity or virtuality, itself a pioneering calculation involving significant ingenuity.
- The effect of each successive order in PT is clear, with the jump from NLO to NNLO much smaller than that from LO to NLO.
- The much-improved scale dependence results in a very accurate theoretical prediction that could even be used as a luminosity monitor at the LHC.

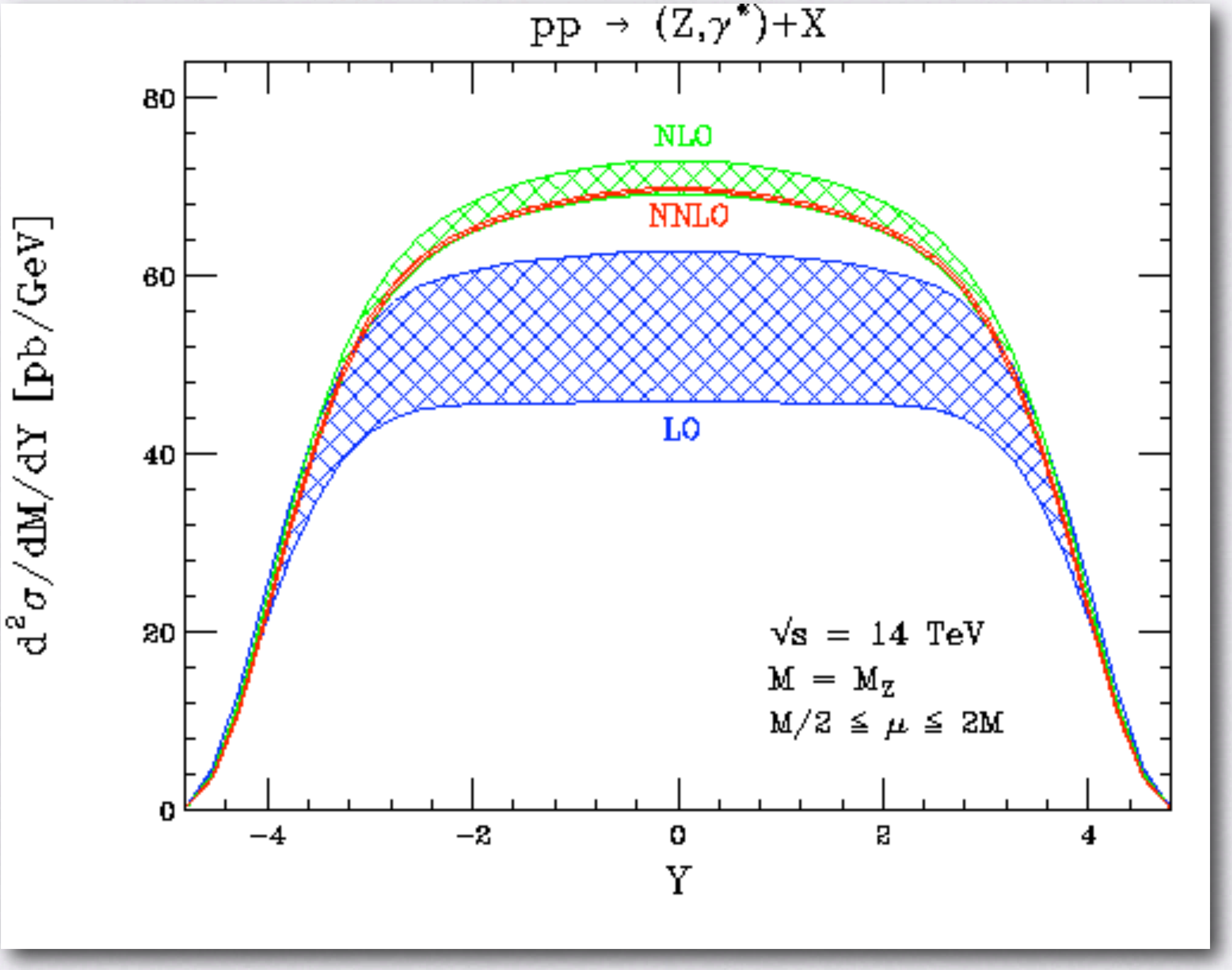

Anastasiou, Dixon, Melnikov, Petriello, 2003.

- The accuracy of the NNLO prediction is demonstrated by a recent measurement of the *Z* rapidity spectrum by D0 at the Tevatron.

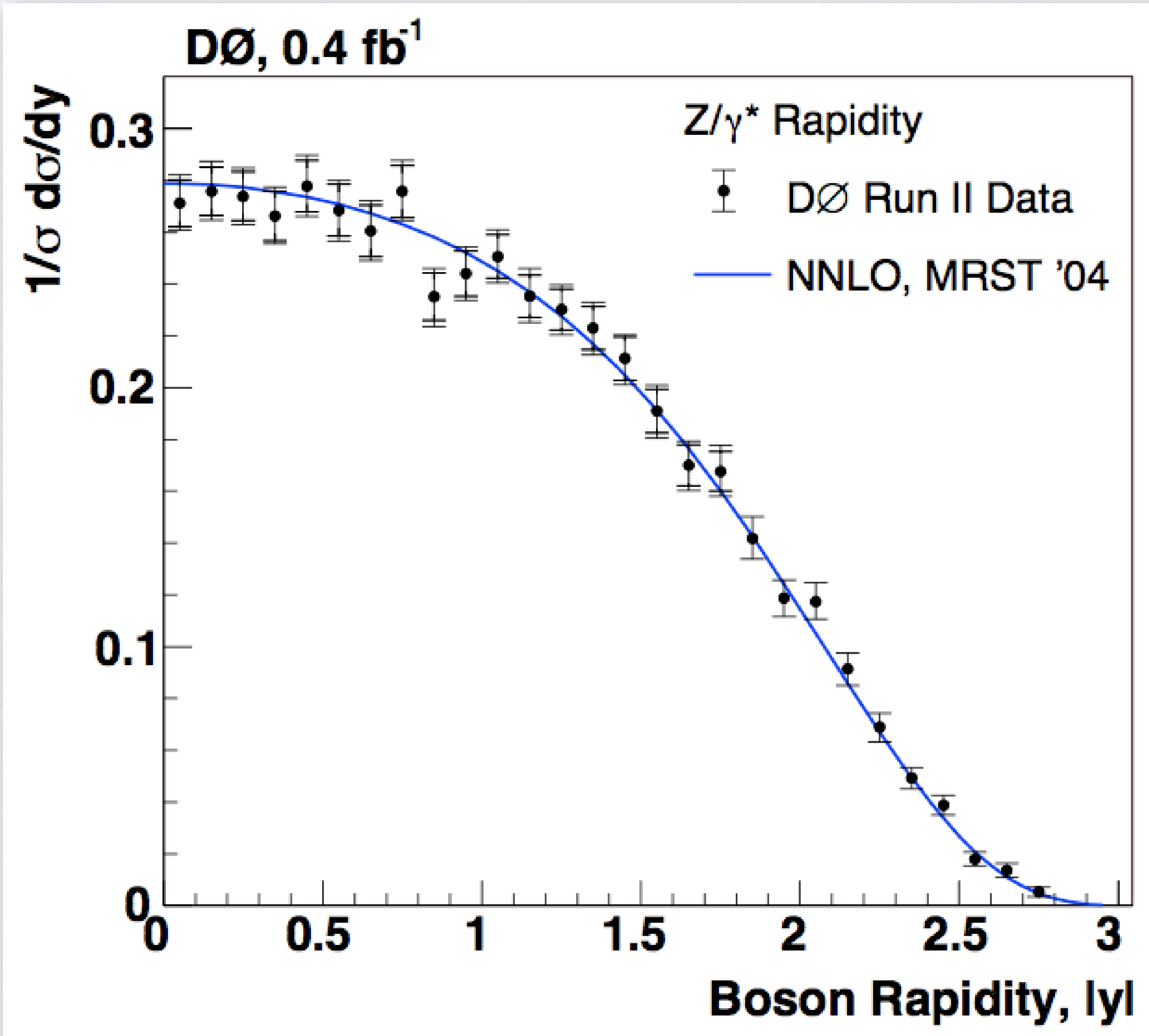

PRD 76, 012003 (2007)

HepCode database

- Further information about some of the tools which I have discussed (as well as others that I haven't had time for) is available at the CEDAR HepCode page.

- The aim is to provide a central repository of information (but not the codes themselves) so that interested experimenters/ phenomenologists can keep abreast of the latest theory predictions available.

- The codes span the breadth of theory approaches available - fixed order, parton showers, calculations with resummation - and pertain to electron-positron, electron-proton and hadron colliders.

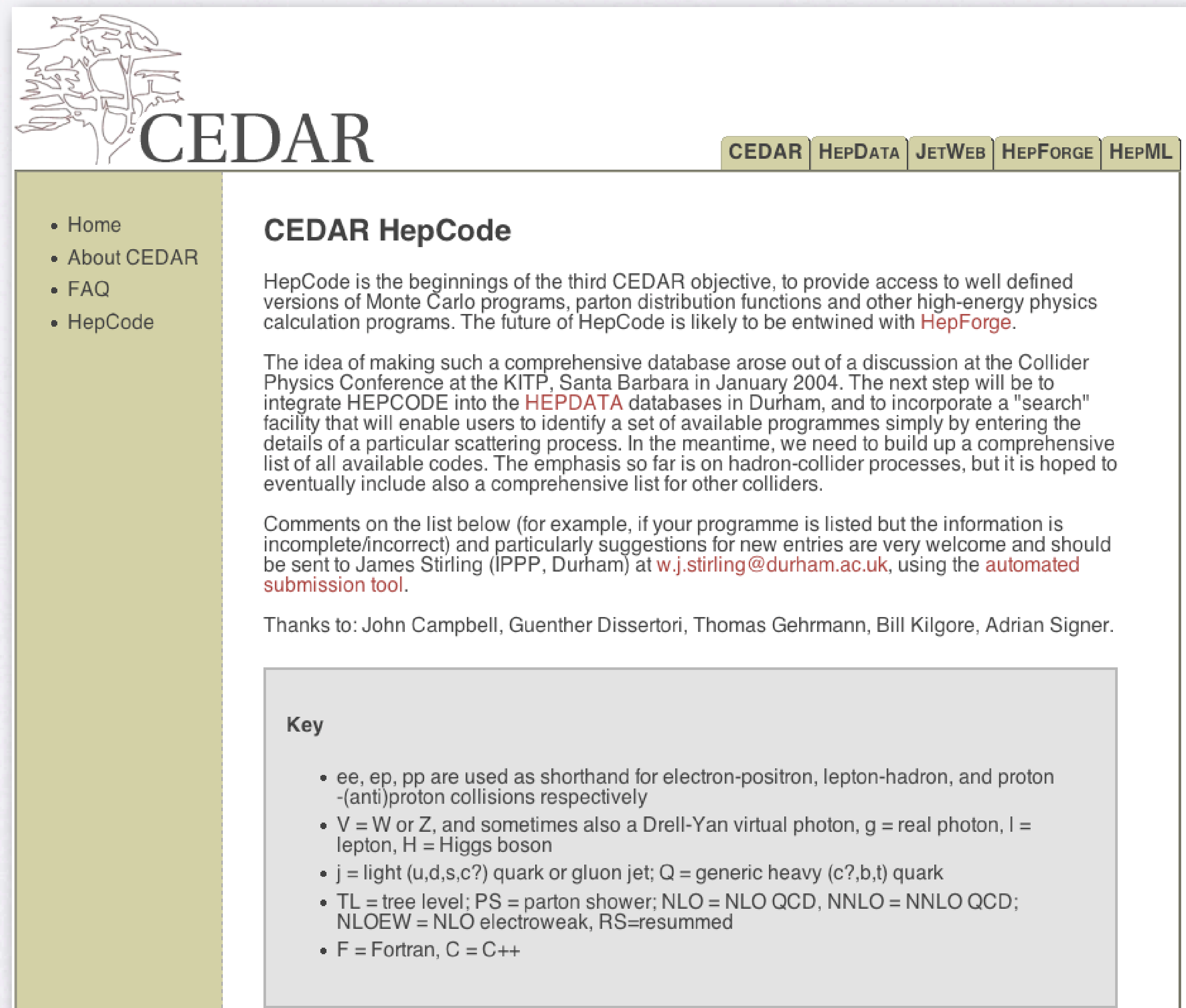

http://www.cedar.ac.uk/hepcode/

Concluding remarks

- Extract from a talk based on a seminal paper of 1981, in which the QCD corrections to the gluonic width of the upsilon were calculated.
- Amusingly accurate summary of the situation today.
- Performing higher-order calculations automatically is still the holy grail.

"Use of existing methods would require the assembly of a small army of Kinoshitas and Lindquists to devote many man-years of effort working on computer programs for many separate processes."

CLNS 81/504
July 1981

QCD CORRECTIONS TO THE GLUONIC WIDTH OF THE Υ MESON

Paul B. Mackenzie* and G. Peter Lepage
Newman Laboratory of Nuclear Studies,
Cornell University, Ithaca, NY 14853

With a coupling constant as large as $\alpha_s \sim 0.15$, really good accuracy cannot be expected from predictions based on only a term or two of the perturbation series. If QCD maintains its status as the only reasonable theory of the strong interactions, corrections beyond the one loop order will eventually have to be calculated for most processes of importance. Such calculations will further clarify the question of renormalization scheme dependence. Since a number of these calculations may be as hard or harder than the most difficult perturbation theory calculation performed to date (the calculation of the eighth order correction to the electron's magnetic dipole moment by Kinoshita and Lindquist[16]), this is a daunting prospect. Use of existing methods would require the assembly of a small army of Kinoshitas and Lindquists to devote many man-years of effort working on computer programs for many separate processes.

Continuing advances in computer hardware and software may make it possible to automate more completely the generation and evaluation of Feynman diagrams. The ideal would be the creation of a master program which for any desired process would generate the graphs, assign the momenta in the loops, evaluate the gamma matrix traces and color algebra, and perform the integrals. Without such a major advance in perturbative methods, the necessary task of pushing calculations to get higher orders will be stupefyingly difficult.

"The ideal would be the creation of a master program which for any desired process would generate the graphs, assign the momenta in the loops, evaluate the gamma matrix traces and colour algebra, and perform the integrals."